AD_____

Award Number: DAMD17-00-1-0476

TITLE: Identification of Structural Domains of ESX Required for Breast Cell Transformation

PRINCIPAL INVESTIGATOR: Arthur Gutierrez-Hartmann, M.D.

CONTRACTING ORGANIZATION: University of Colorado Health Sciences Center
Aurora, Colorado 80045-6508

REPORT DATE: June 2003

TYPE OF REPORT: Annual

PREPARED FOR: U.S. Army Medical Research and Materiel Command
Fort Detrick, Maryland 21702-5012

DISTRIBUTION STATEMENT: Approved for Public Release;
Distribution Unlimited

The views, opinions and/or findings contained in this report are those of the author(s) and should not be construed as an official Department of the Army position, policy or decision unless so designated by other documentation.

20031212 132

REPORT DOCUMENTATION PAGE

Form Approved
OMB No. 074-0188

Public reporting burden for this collection of information is estimated to average 1 hour per response, including the time for reviewing instructions, searching existing data sources, gathering and maintaining the data needed, and completing and reviewing this collection of information. Send comments regarding this burden estimate or any other aspect of this collection of information, including suggestions for reducing this burden to Washington Headquarters Services, Directorate for Information Operations and Reports, 1215 Jefferson Davis Highway, Suite 1204, Arlington, VA 22202-4302, and to the Office of Management and Budget, Paperwork Reduction Project (0704-0188), Washington, DC 20503

1. AGENCY USE ONLY (Leave blank)	2. REPORT DATE	3. REPORT TYPE AND DATES COVERED
	June 2003	Annual (1 Jun 2002 - 31 May 2003)

4. TITLE AND SUBTITLE
Identification of Structural Domains ESX Required for Breast Cell Transformation

5. FUNDING NUMBERS
DAMD17-00-1-0476

6. AUTHOR(S)
Arthur Gutierrez-Hartmann, M.D.

7. PERFORMING ORGANIZATION NAME(S) AND ADDRESS(ES)
University of Colorado Health Sciences Center
Aurora, Colorado 80045-6508

E-Mail: a.gutierrez-hartmann@uchsc.edu

8. PERFORMING ORGANIZATION REPORT NUMBER

9. SPONSORING / MONITORING AGENCY NAME(S) AND ADDRESS(ES)
U.S. Army Medical Research and Materiel Command
Fort Detrick, Maryland 21702-5012

10. SPONSORING / MONITORING AGENCY REPORT NUMBER

11. SUPPLEMENTARY NOTES

12a. DISTRIBUTION / AVAILABILITY STATEMENT
Approved for Public Release; Distribution Unlimited

12b. DISTRIBUTION CODE

13. ABSTRACT (Maximum 200 Words)

ESX encodes an Ets family transcription factor gene that is potentially important in breast cancer because the ESX genomic region (chromosome 1q32.1) is amplified in 50% of early breast cancers and ESX mRNA is over-expressed in human breast ductal carcinoma in situ (DCIS). However, the precise molecular mechanism by which ESX mediates breast cell transformation remains unknown. We have now completed the key milestones originally proposed. Specifcally, we have demonstrated that stable expression of HA-tagged or GFP-tagged ESX transforms the human, non-transformed MCF-12A cell line (which fails to express endogenous ESX). Moreover, we have documented that the subcellular localization of Esx is cytoplasmic, and that it is this subcellular localization that is required for transformation. Indeed, nuclear localization appears to mediate apoptosis. We have excluded the key transcriptional motifs as being required for transformation, and have mapped the transforming Esx subdomain to a small, acidic region. Taken together, these data reveal that Esx is not functioning as a transcription factor to transform MCF-12A mammary cells, but rather that ESX functions primarily via cytoplasmic mechanisms. Finally, we demonstrate that endogenous Esx protein is localized in the cytoplasm in human breast cancer specimens. In summary, these are extremely novel results and challenge dogma that Ets factors must always function in the nucleus as transcription regulators.

14. SUBJECT TERMS
Ets, ESX, transformation, transcription, cytoplasmic

15. NUMBER OF PAGES
71

16. PRICE CODE

17. SECURITY CLASSIFICATION OF REPORT	18. SECURITY CLASSIFICATION OF THIS PAGE	19. SECURITY CLASSIFICATION OF ABSTRACT	20. LIMITATION OF ABSTRACT
Unclassified	Unclassified	Unclassified	Unlimited

Table of Contents

Cover.....1

SF 298.....2

Table of Contents.....3

Introduction.....4

Body.....4

Key Research Accomplishments.....7

Reportable Outcomes.....8

Conclusions.....9

References.....9

Appendices.....10

INTRODUCTION

The Ets family of transcription factors contains several members that are important components of the cellular pathways leading to tumorigenesis (1). For example, several Ets members are downstream targets of oncogenic Ras (2); dominant-negative Ets reverses the transformed phenotype (3,4); and, Ets proteins have been shown to regulate a repertoire of genes that govern cellular survival, proliferation and migration (1,6). Moreover, several Ets factors have been implicated in breast cancer (1,6). However, the ability of Ets factors to transform human breast cells, the identity of the precise Ets factor required for breast cell transformation, and the molecular mechanism by which such an Ets factor mediates breast cell transformation, all remain unknown. The ESX gene is an Ets member that is particularly relevant to breast cancer. ESX is located on chromosome 1q32.1, in a region that is amplified in 50% of early breast cancers. ESX mRNA is over-expressed in human breast ductal carcinoma in situ (DCIS) (7-9). Also, there is a positive feedback loop between the HER2/neu proto-oncogene and ESX, in that HER2/neu activation induces ESX expression, while ESX activates the HER2/neu promoter via a putative ESX DNA binding site (7-9). Finally, HER2/neu and ESX expression levels are positively correlated in human breast cancer cell lines (7-9). Based on these observations, we have chosen to determine whether ESX is capable of transforming immortalized, but non-transformed MCF-12A human breast cells, and to determine the precise mechanism(s) by which ESX transforms these human breast epithelial cells.

BODY

Task 1: To define the modular structural domains of ESX (± DNA) using Cleveland and peptide sequencing analysis.

As noted in our previous Progress Reports, and now presented in a publication (10), we have fully characterized an HA-tagged ESX mammalian expression construct, showing that HA-ESX is expressed as a protein of about ~47 kDa in transiently transfected HeLa and MCF-12A cells. We also characterized the transcription potency and promoter specificity of HA-ESX (10). Taken together, these data revealed that HA-ESX differentially regulates several breast-cancer relevant gene promoters, in particular collagenase and HER2/neu.

We also generated ESX as a fusion protein with GST, and we have optimized conditions to express recombinant GST-ESX in bacteria and to purify it to homogeneity. Having made GST-ESX containing a thrombin cleavage site between GST and ESX, we also optimized conditions for cleavage of ESX from GST-ESX immobilized on glutathione beads. While this approach has been releasing intact ESX, the amounts released were initially very low (~2-5% of total). We have now optimized the expression and purification of ESX devoid of the GST leader in an efficient manner. Finally, we have also subcloned defined, but overlapping, regions of ESX into a bacterial expression vector with the long term goals of producing recombinant ESX fragments as affinity matrices for protein purification (see Task 3) and for region-specific antibody development.

Using the highly purified, full-length recombinant GST-ESX, we generated rabbit polyclonal anti-ESX antibodies, in collaboration with ABR, Inc., in Golden, CO, as originally proposed.

These antibodies, which are very important reagents, are now commercially sold by ABR to the entire scientific community, thus providing an invaluable research tool to all breast cancer investigators. We have characterized these anti-ESX antibodies and shown that they recognize a ~47 kDa nuclear protein that is expressed in T47D breast cancer cells. Importantly, we also documented that ESX is not expressed in the non-transformed human MCF-12A mammary cell line (11). Additionally, these anti-ESX antibodies have already been very useful in measuring ESX protein expression levels in the transcription and transformation assays, as described above. We also initiated a new project with these anti-ESX antibodies and we have optimized the chromatin immunoprecipitation (ChIP) assay to show that ESX actually binds to certain cellular target genes in vivo, during the initial stages of ESX expression (12).

We have used these anti-ESX antibodies in immuno-histochemical (IHC) analysis of ESX expression in primary human breast cancer specimens and immuno-cytochemical (ICC) analysis of T47D (ESX^+), MCF-12A (ESX^-) and MCF-12A (ESX^+) human mammary cell lines (12). In collaboration with Dr. Menakshi Singh, in our Pathology Dept., we show that endogenous ESX is primarily located in the cytoplasm in primary human breast cancer specimens and T47D breast cancer cell line (12). By contrast, no ESX protein was detected in the control MCF-12A cells, whereas ESX was detected primarily localized to the nucleus in MCF-12A cells transiently transfected with an HA-ESX expression vector (12). These data suggest differential localization of ESX in malignant (cytoplasmic) cell lines and tissues vs nonmalignant (nuclear) cell lines, and our most recent report verifies this point as a novel mechanism of mammary cell transformation mediated by a putative transcription factor.

Finally, while we initially pursued the Cleveland digestion protocol ± DNA, as originally described in our proposal, as our studies progressed we realized that ESX transforms cells via a cytoplasmic mechanism and not via a nuclear, transcription-mediated mechanism. For this reason, we halted these studies for now, and decided to pursue the more physiologically-relevant studies in Tasks 2 and 3.

Task 2: To define the modular domain of ESX required for breast cell transformation.

These studies turned out to be the most informative of all, and the results are strikingly novel! We have made several important discoveries about the role of ESX in breast epithelial cell proliferation and transformation, and the data are detailed in three manuscripts (10-12). First of all, we have completed the preliminary studies showing that transient expression of HA-ESX and HA-VP16-ESX in MCF-12A cells results in increased colony formation (10). Using a colony formation assay, we found that HA-ESX and HA-Ets-2 mediated MCF-12A cell colony formation rates that approached those generated by oncogenic V12 Ras, whereas empty vector had a negligible effect. By contrast, in immortalized and transformed T47D breast cancer cells, which express abundant amounts of HER2/neu and ESX, we found that anti-sense and dominant-negative HA-ESX inhibited T47D colony formation, whereas control vector allowed formation of many colonies.

In the second report (11), we show that we have established a number of MCF-12A cell lines stably expressing either vector control HA-ESX, HA-VP16-ESX, HA-ETS-2, or V12-Ras. We chose the MCF-12A cell line because it is immortalized, but nontransformed, and importantly these cells fail to express endogenous ESX protein. We used pCGN2-HA-Ets-2 and pSVRas expression vectors as positive controls for transformation. Stable expression of ESX induced EGF-independent proliferation, serum-independent MAPK phosphorylation and growth in soft agar. Additionally, stable ESX expression conferred increased cell adhesion, motility and invasion in two-dimensional and trans-well filter assays. An epithelial to mesenchymal morphological transition was noted in stable ESX cells. In three-dimensional cultures, parental and control (pCGN2) cells formed highly organized duct-like structures with evidence of cell polarity, ECM adhesion-dependent proliferation and cell survival, and lack of cellular invasion into surrounding matrix. Remarkably, the ESX stable cells formed solid, disorganized structures, with lack of cell polarity and loss of dependence on ECM adhesion for cell proliferation and survival. In addition, ESX cells invaded the surrounding matrix, indicative of a transformed and metastatic phenotype. The positive control cell lines, HA-Ets-2 and V12Ras, also increased adhesion, motility and invasion, while displaying differences in cellular morphology. Finally, the negative control (pCGN2) cells lacked any evidence of the transformed and EMT phenotypes.

These studies have been completed in collaboration with Dr. Pepper Schedin of the AMC Cancer Center here in Denver, and this Ms. detailing these results has been accepted by *Oncogene* (see Appendix). This study establishes ESX and Ets-2 as putative oncogenes capable of conferring the transformed phenotype to otherwise normal MCF-12A human mammary epithelial cells.

In the third paper, we have focused on mapping the subdomain of ESX that is necessary and sufficient for transforming MSF-12A cells, using GFP-fusions of ESX sub-regions and colony formation in soft agar as the key assays. Specifically, since we had not been able to detect HA-ESX protein in the MCF-12A cells stably transfected with the HA-ESX expression vector, we were unable to determine its subcellular localization, despite the fact that HA-ESX actually transformed these human mammary cells. However, the cytoplamic localization of ESX in the T47D breast cancer cell lines and primary tissues forced us to re-consider our original hypothesis and also forced us to more carefully analyze the subcellular localization of ESX. To this end, we constructed a GFP-ESX fusion and generated multiple distinct pools of MCF-12A cells stably expressing this construct. Real-time GFP-ESX expression in living cells was followed on a daily basis using fluorescence microscopy during the G418 selection process. These studies revealed that GFP-ESX is initially robustly expressed in the nucleus in most cells, and in the cytoplasm in fewer cells. After about 28-30 hours, the cells expressing GFP-ESX in the nucleus die by apoptosis, and the population expressing GFP-ESX in the cytoplasm persist and become the dominant and ultimately transformed cell population.

To map the region of ESX required for MCF-12A cell transformation, we fused various ESX constructs that had been internally deleted of key functional domains (eg, Pointed, TAD, acidic/Sox and Ex7/NLS domains) to GFP. The data reveal that deletion of any domain invovld with either nuclear localization (Ex7/NLS) or transcription (Pointed or TAD), did not

interfere with the transforming potential of ESX in the soft agar colony formation assay. By constrast, internal deletion of the 40-AA acidic/Sox domain resulted in complete loss of ESX's transforming ability. Furthermore, adding a strong NLS to either the WT or the Ex7/NLS-deleted ESX constructs resulted in loss of transformation ability. Finally, to determine whether the 40-AA acidic/Sox domain is necessary and sufficient for transformation, we fused this short region alone to GFP and documented that it resulted in robust colony formation in soft agar in a manner equivalent, if not better, than the full-length ESX version. Furthermore, appending an NLS signal to the 40-AA acidic/Sox domain reversed its transforming capability, again proving that nuclear localization is incompatible with its ability to transform MCf-12A cells (12).

Task 3: To identify the proteins that associate with the ESX transforming domain using MALDI-TOF.

As noted above, our more recent discovery that endogenous ESX is localized primarily to the cytoplasm in human breast cancer specimens and in the T47D breast cancer cell line, and that cytoplasmic expression of the 40-AA transforming ESX motif is sufficient for transformation, we have had to reassess our original hypothesis. We originally hypothesized that ESX main function was as a transcription factor, however, it has now become clear that it functions primarily in the cytoplasm. Thus, the overall approach to this Aim remains essentially unchanged, except that we will focus on purifying cytoplasmic proteins that bind to the ESX transforming 40-AA domain. In this regard, we have already generated multiple GST-ESX fusion constructs, including one that contains the 40-AA acidic Sox domain. Moreover, we have initiated affinity chromatography purification steps using this GST-40AA(Acidic/Sox domain), in order to purify cytoplasmic proteins that bind to this transforming motif. The proteins will be separated using SDS-PAGE, the protein bands cut out and then submitted to MALDI-TOF mass spectrometry for identification. Preliminary data are encouraging.

KEY RESEARCH ACCOMPLISHEMENTS

- Establishment of multiple pools of MCF-12A cells stably expressing HA-ESX, HA-VP16-ESX, HA-Ets2, V12-Ras or vector control.
- Documenting that ESX and Ets-2 function as oncogenes and transform MCF-12A human mammary cells, resulting in a functional epithelial-to-mesenchymal transformation (EMT) phenotype.
- Showing that endogenous ESX is localized to the cytoplasm in human breast cancer specimens and T47D breast cancer cell lines, using IHC and ICC, respectively.
- Establishment of GFP-ESX stable pools in MCF-12A cells and discovering that GFP-ESX is primarily localized in the cytoplasmic subcellular region.
- Generating GFP-ESX internal deletions and defined domain fusion constructs, and establishing pools of MCF-12A cells stably expressing each of these constructs.
- Using these constructs to show that cytoplasmic expression of a 40-AA acidic/Sox domain is necessary and sufficient for MSF-12A cellular transformation.

REPORTABLE OUTCOMES

Abstracts:

(1) Identification of ESX-Regulated Genes that Promote Breast Cell Transformation by cDNA Microarray Analysis, G.J. Cappetta, Kristin Eckel, Arthur Gutierrez-Hartmann, University of Colorado Health Sciences Center, Denver, CO. National Endocrine Society Meeting, Denver, CO, June, 2001.

(2) Analysis of ESX Function in the Development of Human Breast Cancer. J.D. Prescott, A. Gutierrez-Hartmann, University of Colorado Health Sciences, Denver, CO. National Endocrine Society Meeting, Denver, CO, June, 2001.

(3) The ESX Transcription Factor in Human Breast Cancer: Localization of the ESX Protein in Human Breast Epithelial Cells and Identification of Her-2 as an ESX Target Gene. J.D. Prescott, M. Singh, A. Gutierrez-Hartmann, University of Colorado Health Sciences, Denver, CO. National Endocrine Society Meeting, San Francisco, CA, June, 2002.

(4) ESX induces transformation and functional epithelial to mesenchymal transition in MCF-12A mammary epithelial cells. P.J. Schedin, K.L. Eckel, S.M. McDaniel, K.S. Brodsky, J.J. Tentler, A. Gutierrez-Hartmann, AMC Cancer Research Center, Denver, CO; University of Colorado Health Sciences Center, Denver, CO. American Association for Cancer Research Meeting, San Francisco, CA, 2002.

(5) The Ets Transcription Factor ESX Directly Activates Expression of the HER-2 Proto-oncogene. J.D. Prescott & A. Gutierrez-Hartmann, University of Colorado Health Sciences, Denver, CO. San Antonio Breast Cancer Symposium Abstract, 2002.

(6) Cytoplasmic expression of ESX is required for MSF-12A transformation. J.D. Prescott, K. Koto, M. Singh, A. Gutierrez-Hartmann, University of Colorado Health Sciences Center, Denver, CO. American Association for Cancer Research Meeting, Washington, DC, 2003.

Manuscripts

(1) Eckel KL, Tentler JT, Cappetta GJ, Diamond SE and Gutierrez-Hartmann A. (2003) The epithelial-specific ETS transcription factor ESX/ESE-1/Elf-3 modulates malignancy-associated gene expression and breast cell growth. *DNA & Cell Biol.* 22:79-94..

(2) Schedin PJ, Eckel KL, McDaniel SM, Brodsky KS, Tentler JT, Prescott JD and Gutierrez-Hartmann A. ESX Induces transformation and functional epithelial to mesenchymal transition in MCF-12A mammary epithelial cells. Oncogene, in press.

(3) Prescott JD, Koto K, Singh M, Gutierrez-Hartmann A. Cytoplasmic expression of an acidic 40-amino acid region of ESX transcription factor defines a novel mammary transformation mechanism. In preparation.

Reagents Developed

(1) Rabbit polyclonal anti-ESX antibodies now commercialized by ABR, Inc., Golden, CO.

Funding applied for and received based on this work

(1) J.D. Prescott, National DOD Pre-doctoral Award, 6/2001: Awarded, 6/2002.

CONCLUSIONS

The 3-year support provided by the DOD/DAMD Idea Award has been critical in allowing us to pursue ESX as a putative mediator mammary cell transformation and of ESX as clinical target in breast cancer. Using this support, we have made several critical and very innovative discoveries regarding ESX and mammary tumorigenesis that is very likely to impact the clinic. Specifically, we have shown that while ESX is an Ets-family transcription factor that is capable of acting as a nuclear regulator of gene expression in transient transfection reporter assays, that this is not the physiologically-relevant mode of ESX action. We used a variety of techniques to show that stable expression of ESX in MCF-12A cells results in all the hallmarks of cellular transformation and an epithelial-to-mesenchymal transition. Furthermore, we carefully showed that stable expression occurs in the cytoplasm and that nuclear targeting of ESX (or its subdomains) reverses the transformed phenotype. Finally, we mapped the transforming ESX domain to a 40-AA highly acidic motif that haas been reported to be similar to the Sox domain, and we showed that the cytoplasmic expression of this motif is necessary and sufficient for MSF-12A cellular transformation. While we do not yet understand the mechanism by which this 40-AA domain mediates cellular transformation, we do know that it is initially via cytoplasmic effectors. This is in striking contrast with its known structure as a transcription factor of the Ets-family, wherein it would be expected to function via regulation of promoter activity. Finally, given that endogenous ESX is expressed cytoplasmically in human breast cancer, these issue become very clinically relevant. Ultimately, we anticipate that these studies will provide a novel marker and several new drug targets to use in our battle against breast cancer.

REFERENCES

1. Wasylyk, B, and Nordheim, A. 1997. Ets transcription factors: Partners in the integration of signal responses., p. 251-284. *In* A. Papavassiliou (ed.), Transcription Factors in Eukaryotes. Landes Bioscience.
2. Wasylyk, B, Hagman, J, and Gutierrez-Hartmann, A. 1998. Ets transcription factors: nuclear effectors of the Ras/MAP kinase signaling pathway. Trends Biochem. Sci. 23:213-216.
3. Sapi, E, Flick, M, Rodov, S, and Kacinski, B. 1998. Ets-2 transdominant mutant abolishes anchorage-independent growth and anchorage-stimulating factor-stimulated invasion by BT20 breast carcinoma cells. Cancer Res. 58:1027-1033.
4. Delannoy-Courdent, A, Mattot, V, Fafeur, V, Fauquette, W, Pollet, I, Calmels, T, Vercamer, C, Boilly, B, Vandenbunder, B, and Desbiens, X. 1998. The expression of Ets-1 transcription factor lacking its activation domain decreases uPA proteolytic activity and cell motility, and impairs normal tubulogenesis and cancerous scattering in mammary epithelial cells. J. Cell Sci. 111:1521-1534.
5. Galang, C, Garcia-Ramirez, J, Solski, P, Westwick, J, Der, C, Neznanov, N, Oshima, R, and Hauser, C. 1996. Oncogenic Neu/ErbB-2 increases, Ets, AP-1 and NF-kB-dependent gene expression, and inhibiting Ets activation blocks Neu-mediated cellular transformation. J. Biol. Chem. 271:7992-7998.
6. Janknecht, R, and Nordheim, A. 1993. Gene regulation by Ets proteins. Biochim. Biophys. Acta 1155:346-356.

7. Chang, C, Scott, G, Kuo, W, Xiong, X, Suzdaltseva, Y, Park, J, Sayre, P, Erny, K, Collins, C, Gray, J, and Benz, C. 1997. ESX: A structurally unique Ets overexpressed early during human breast tumorigenesis. Oncogene 14:1617-1622.
8. Oettgen, P, Alani, R, Barcinski, M, Brown, L, Akbarali, Y, Boltax, J, Kunsch, C, Munger, K, and Libermann, T. 1997. Isolation and characterization of a novel epithelium-specific transcription factor, ESE-1, a member of the *ets* family. Mol. Cell. Biol. 17:4419-4433.
9. Tymms, M, Ng, A, Thomas, R, Schutte, B, Zhou, J, Eyre, H, Sutherland, G, Seth, A, Rosenberg, M, Papas, T, Debouck, C, and Kola, I. 1997. A novel epithelial-expressed ETS gene, ELF3: Human and murine cDNA sequences, murine genomic organization, human mapping to 1q.32.2 and expression in tissues and cancer. Oncogene 15:2449-2462.
10. Eckel, KL, Tentler, JT, Cappetta, GJ, Diamond, SE, Gutierrez-Hartmann A. 2003. The epithelial-specific ETS transcription factor ESX/ESE-1/Elf-3 modulates breast cancer-associated gene expression. *DNA & Cell Biol.* 22:79-94.
11. Schedin PJ, Eckel KL, McDaniel SM, Prescott JD, Brodsky KS, Tentler, JJ, Gutierrez-Hartmann, A. (2003) ESX induces transformation and functional epithelial to mesenchymal transition in MCF-12A mammary epithelial cells. *Oncogene, In press.*
12. Prescott, JD, Koto, K, Singh, M, Gutierrez-Hartmann, A. Cytoplasmic expression of an acidic 40-amino acid region of ESX transcription factor defines a novel mammary transformation mechanism. In preparation.

APPENDICES

Enclosed is a copy of our first publication(Eckel et al) and a draft of our second Ms. (Schedin et al) that has been accepted to *Oncogene*.

Eckel KL, Tentler JT, Cappetta GJ, Diamond SE and Gutierrez-Hartmann A. (2003) The epithelial-specific ETS transcription factor ESX/ESE-1/Elf-3 modulates malignancy-associated gene expression and breast cell growth. *DNA & Cell Biol.* 22:79-94..

Schedin PJ, Eckel KL, McDaniel SM, Brodsky KS, Tentler JT, Prescott JD and Gutierrez-Hartmann A. ESX Induces transformation and functional epithelial to mesenchymal transition in MCF-12A mammary epithelial cells. *Oncogene*, in press.

DNA AND CELL BIOLOGY
Volume 22, Number 2, 2003
© Mary Ann Liebert, Inc.
Pp. 000–000

The Epithelial-Specific ETS Transcription Factor ESX/ESE-1/Elf-3 Modulates Breast Cancer-Associated Gene Expression

KRISTIN L. ECKEL, JOHN J. TENTLER, GERALD J. CAPPETTA, SCOTT E. DIAMOND,[1] and ARTHUR GUTIERREZ-HARTMANN

ABSTRACT

Several members of the ETS family of transcription factors contribute to tumorigenesis in many different tissues, including breast epithelium. The ESX gene is an epithelial-specific Ets member that is particularly relevant to breast cancer. ESX is amplified in early breast cancers, it is overexpressed in human breast ductal carcinoma *in situ*, and there may be a positive feedback loop between the HER2/neu proto-oncogene and ESX. Despite this progress in our understanding of ESX, its ability to regulate tumor-related gene expression and to modulate breast cell survival, remain unknown. Here we show that HA-ESX stimulates the collagenase and HER2/neu promoters, but fails to activate an intact stromelysin promoter. However, HA-ESX activates, in a dose-dependent manner, a heterologous promoter containing eight copies of the Ets binding site derived from the stromelysin gene (p8Xpal-CAT). Analysis of the ability of constructs encoding nine Ets family members to activate the HER2/neu promoter revealed three patterns of gene activation: (1) no effect or repressed promoter activity (Elk-1 and NET); (2) intermediate activity (ER81, GABP, ESX, and HA-Ets-2); and, (3) maximal activity (Ets-1, VP-16-Ets-1, and EHF). Based on these observations, we also determined whether ESX is capable of conferring a survival phenotype upon immortalized, but nontransformed and ESX negative MCF-12A human breast cells. Using a colony formation assay, we found that HA-ESX and HA-Ets-2, mediated MCF-12A cell survival rates that approached those generated by oncogenic V12 Ras, whereas empty vector resulted in negligible colony formation. By contrast, in immortalized and transformed T47D breast cancer cells, which express both HER2/neu and ESX, we found that antisense and dominant-negative HA-ESX inhibited T47D colony formation, whereas control vector allowed formation of many colonies. These results are significant because they show that HA-ESX is able to differentially activate several malignancy-associated gene promoters, and that ESX expression is required for cellular survival of nontransformed MCF-12A and transformed T47D human mammary cells.

INTRODUCTION

THE ETS FAMILY OF TRANSCRIPTION FACTORS represents a class of *trans*-acting phosphoproteins with important roles in cell proliferation, differentiation, and oncogenic transformation (Bradford and Gutierrez-Hartmann, 1998; Dittmer and Nordheim, 1998; Graves and Petersen, 1998; Wasylyk *et al.*, 1998). The family is defined by the ETS domain, a highly conserved DNA-binding domain (DBD) comprised of ~85 amino acids that is folded into a novel winged helix-turn-helix DNA-binding motif (Donaldson *et al.*, 1994, 1996). Ets proteins function almost exclusively via specific protein–protein interactions, with specific Ets/protein partner combinations binding to bipartite DNA elements on relevant gene promoters (Donaldson *et al.*, 1994, 1996). Thus, the target gene selectivity of Ets factors is greatly influenced by specific protein partners.

The v-*ets* oncogene in the E26 retrovirus causes hematopoetic malignancies in chickens (Leprince *et al.*, 1983). In mam-

Departments of Medicine and of Biochemistry & Molecular Genetics, Program in Molecular Biology, and Colorado Cancer Center, University of Colorado Health Sciences Center, Denver, Colorado.
[1]Current address: Department of Physiology, University of Kentucky College of Medicine, MS-508, Albert B. Chandler Medical Center, 800 Rose Street, Lexington, KY 40536-0298.

malian cells, Ets proteins are not only key nuclear targets of Ras oncogene signaling pathways, but are also required to *trans*-activate a subset of genes that initiate cellular transformation. Ets factors, typically acting via the AP-1/Ets Ras response element (RRE), regulate a wide repertoire of genes that control cell survival (anti-apoptosis), proliferation, and motility, such as: the HER2/neu (Scott *et al.*, 1994), β-integrin (Takaoka et al., 1998; Oda *et al.*, 1999), E-cadherin (Gilles *et al.*, 1997; Rodrigo *et al.*, 1999), Bcl-XL (Sevilla *et al.*, 1999), cyclin D (Albanese *et al.*, 1995; Tetsu and Mccormick, 1999), Fos (Treisman, 1992; Wasylyk *et al.*, 1998), Myc (Roussel *et al.*, 1994), Ets (Ets-1/2, Pea-3, ESX) (Baert *et al.*, 1997; Benz *et al.*, 1997; Wasylyk and Nordheim, 1997; Dittmer and Nordheim, 1998; Neve *et al.*, 1998; O'hagan and Ja, 1998), matrix metalloproteinases (Gilles *et al.*, 1997; Watabe *et al.*, 1998; Oda *et al.*, 1999) and maspin (Zhang *et al.*, 1997) genes. Moreover, Ets-induced malignancies are often due to Ets overexpression or gene translocations resulting in chimeras in which the Ets DBD combines with other activation domains (Dittmer and Nordheim, 1998). Although these data strongly implicate Ets factors and Ets target genes in tumorigenesis and metastasis, the ability of the *c-Ets-1* and *c-Ets-2* proto-oncogenes to transform NIH 3T3 fibroblasts is actually negligible, and may require a previous "hit" (Seth and Papa, 1990; Galang *et al.*, 1994; Robinson *et al.*, 1997).

The most compelling data supporting a direct role of Ets proteins in mammary tumorigenesis has been the ability of the dominant-negative (dn) Ets-2 DBD to completely block the anchorage-independent growth and cellular invasiveness of NmuMG, MMT, and BT20 breast carcinoma cells (Delannoy-Courdent *et al.*, 1998; Sapi *et al.*, 1998). The dn-Ets protein functions as a dominant inhibitory effector by competing with endogenous, intact Ets factors for Ets binding sites on target genes (Langer *et al.*, 1992; Wasylyk *et al.*, 1994; Bradford *et al.*, 1995, 1996, 1997; Galang *et al.*, 1996; Foos *et al.*, 1998). Moreover, several specific Ets proteins, including members of the ETS-1, PEA-3, and ESX subfamilies, are upregulated in breast tumorigenesis (Baert *et al.*, 1997; Benz *et al.*, 1997; Gilles *et al.*, 1997; Watabe *et al.*, 1998). Although these studies clearly implicate Ets factors in breast cancer, the ability of a specific Ets factor to affect survival or transformation of normal breast cells has not been shown.

ESX (*e*pithelial-restricted with *s*erine bo*x*), also known as Jen, ERT, ELF-3, or ESE-1, is a novel, epithelial-specific human Ets factor that is unique among Ets factors in several respects (Andreoli *et al.*, 1997; Chang *et al.*, 1997; Oettgen *et al.*, 1997; Tymms *et al.*, 1997; Choi *et al.*, 1998). First, its expression is restricted to the most terminally differentiated epithelial-derived cells in the colon, prostate, kidney, uterus, skin, pancreas, stomach, trachea, fetal lung, and the mammary gland (Oettgen *et al.*, 1997; Neve *et al.*, 1998). Second, ESX contains not only the usual Pointed (PNT) and ETS DBD domains found in many Ets factors, but also contains a Sox-like serine-rich box and an HMG-like AT-hook domain (Fig. 1) (Chang *et al.*, 1997; Oettgen *et al.*, 1997, 1999; Tymms *et al.*, 1997; Choi *et al.*, 1998).

F1

ESX is of particular relevance to breast cancer. ESX expression in normal breast increases in the epithelium of ductules and terminal ductal-lobular units during ductal development, then declines throughout terminal differentiation, and is then reexpressed dramatically during glandular involution (Neve *et al.*, 1998). Thus, ESX expression in normal breast may be involved in the restructuring and involution processes of the mammary gland, and aberrant ESX expression may alter these normal breast remodeling processes and result in tumorigenesis (Neve *et al.*, 1998). Indeed, ESX is abundantly expressed in human mammary epithelial carcinomas (Chang *et al.*, 1997; Tymms *et al.*, 1997). Moreover, the ESX gene maps to human chromosome 1q32.1, in a region that is overrepresented in 50% of early breast cancers (Chang *et al.*, 1997; Tymms *et al.*, 1997). Additionally, ESX is overexpressed in human breast ductal carcinoma *in situ* (DCIS) (Chang *et al.*, 1997); an early cancer stage that also overexpresses HER2/neu (Liu *et al.*, 1992). A positive feedback loop between the HER2/neu proto-oncogene and ESX appears to exist in human breast cancer cell lines (Chang *et al.*, 1997; Neve *et al.*, 1998). Thus, taken together, these data show that ESX is a critical gene target of the HER2/neu pathway, and suggest that ESX expression may be necessary to achieve the particularly malignant phenotype associated with HER2/neu.

Here we show that HA epitope-tagged ESX stimulates certain metalloproteinase genes and the HER2/neu promoter, and that the HER2/neu promoter is differentially activated by constructs encoding nine distinct Ets transcription factors. Most importantly, we show that HA-ESX and HA-Ets2 are able to confer a survival phenotype to MCF-12A human breast cells with equal potency as oncogenic V12Ras, and that antisense and dominant-negative HA-ESX inhibited T47D colony formation. These results are significant because they are the first demonstration that ESX, a member of the Ets family of transcription factors, is required for colony formation of nontransformed human mammary cells.

MATERIALS AND METHODS

ESX mammalian expression vectors

A cDNA spanning the coding sequence of human ESX mRNA was amplified by RT-PCR using oligonucleotides di-

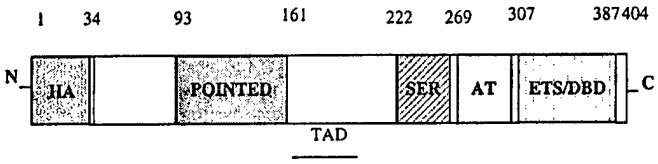

FIG. 1. Schematic structure of HA-tagged human ESX protein. ESX coding sequence includes an amino-terminal (N) pointed domain (POINTED), the serine box (SER), an A/T hook region (AT), and a carboxy-terminal (C)ETS DNA binding domain (DBD).

rected to the 5′ and 3′ ends of the ESX open reading frame, to produce an ESX DNA product flanked by *BamH* I and *EcoR* I sites for later subcloning. The ESX oligonucleotide sequences used were: 5′cgagatctccggaattcatATGGCTGCAACCTGTGA and 5′tccagagtcggaactgaatGAATTCCGGAGATCTCG, with the capital letters indicating ESX sequences and underlined bases representing the ATG in the first sequence. Amplified ESX cDNA was subcloned into pCR2.1 (Invitrogen Corporation, San Diego, CA) to yield pCR2.1-ESX plasmid DNA. The ESX sequence and its orientation was verified by dideoxy sequencing by the UCHSC Cancer Center DNA Sequencing Core facility. Plasmid pCR2.1-ESX was used as the source of ESX DNA for the construction of a variety of mammalian ESX expression vectors. Thus, ESX was excised from pCR2.1-ESX by digestion with *EcoR* I and ligated to the unique *EcoR* I site of mammalian expression vector pCDNA3.1 (Invitrogen Corporation) to generate pCDNA3.1-ESX. Similarly, pCR2.1-ESX was digested with *Bgl* II and *Afl* III, and the 1116 base pair *Bgl* II ESX fragment was ligated into a *BamH* I linearized and dephosphorylated pCGN2-HA vector (Tanaka and Herr, 1994; Gordon *et al.*, 1997; Bradford *et al.*, 2000) to generate pCGN2-HA-ESX. Construction of the dominant-negative version of ESX was accomplished in two cloning steps. First, the ESX AT-hook and DNA-binding domain was PCR amplified from pCR2.1-ESX, using an oligonucleotide that included a Kozak consensus site (lower case), followed by an initiator methionine (bold), an in-frame HA epitope tag (italics) and a five amino acid linker (underlined) fused to amino acid 229 of ESX: 5′ccacc**ATG***GCTTCTTATCCTTATGACGTGCCTGACTAT*-GCCAGCTCGGGACCTGATGGTTTTGGTGAC 3′. The same 3′ primer that was used for the construction of pCR2.1-ESX was also used for the amplification of the ESX DBD region. The PCR product was cloned into pCR2.1, and the DNA sequence was verified by the UCHSC core sequencing facility. In the second cloning step, the HA-ESX DBD cDNA was excised from pCR2.1-ESX DBD with *EcoR* V and *Spe* I and subcloned into pCDNA3.1 at the *EcoR* V and *Xba* I sites, resulting in a dominant-negative version of ESX (pCDNA3.1-HA-ESX DBD).

Reporter constructs

The 1100-CAT and 550-CAT, contain 1100 and 550 bp of upstream promoter sequences derived from the rat stromelysin gene, respectively, and have been described previously (Wasylyk *et al.*, 1991). The −517pBLCAT collagenase construct contains the −517 to +63 region of the human collagenase gene cloned in the pBLCAT plasmid (Angel *et al.*, 1987). The pA3Her2/neu-Luc reporter was constructed by first amplifying the −582 to +30 region of the human Her2/neu promoter region from HeLa genomic DNA using the following primers (Gibco/BRL Gaithersburg, MD): 5′ AAGTCCTTTCGATGAGACT 3′ and 5′ AAGCTTCTGGTTTCTCCGGTCCCAATGGA 3′. This 612-bp fragment, which included an internal, genomic Sma I site at position, was cloned in to pCR-2.1. Once its DNA sequence was verified, a 527-bp fragment spanning positions −497 to +30, was excised from pCR2.1-Her2/neu and then ligated directionally into the *Hind* III and *Sma* I sites of the luciferase based reporter vector, pA3luc (Maxwell *et al.*, 1989).

Construction of HA-ESX expression vector

The human ESX gene consists of nine exons and eight introns that span approximately 4 kb of DNA on chromosome 1q32, and encodes a 371 amino acid protein product that is reported to be 42 kDa in mass (Chang *et al.*, 1997). The ESX protein is comprised of multiple functional domains, including an N-terminal pointed (PNT) domain, a serine box, an AT-rich region, and a C-terminal ETS DNA-binding domain (ETS-DBD) (Fig. 1). Additionally, deletion analysis has identified a highly acidic *trans*-activation domain (TAD) spanning amino acids 129 and 159 (Chang *et al.*, 1999). To study the transcription and growth-promoting properties of ESX, full-length ESX was amplified by RT-PCR from T47D mRNA and then amino-terminally tagged with the hemagglutinin (HA) epitope by cloning into the pCGN2 mammalian expression vector (pCGN2-HA-ESX, Fig. 1) (Gordon *et al.*, 1997; Bradford *et al.*, 2000). The HA epitope tag was included to monitor exogenous ESX expression levels and to distinguish between recombinant ESX and the endogenous protein.

Ets factor and Ras effector plasmids

Ets factor plasmids pTL1-Elk-1, pSG5-Ets-1, pSG5-VP16-Ets-1, and pTL2-hNet constructs were provided by Bo Wasylyk (IGBMC, Illkirch, France) and the HA-tagged Ets-2 (pCGN-HA-Ets-2) was provided by Michael Ostrowski (Ohio State University). EHF, ER81, and GABP plasmid constructs were provided by Frank Burton (University of Minnesota), Ralf Janknecht (The Salk Institute) and Tom Brown (Pfizer, Inc.), respectively. Plasmid pSV-Ras contains oncogenic V12-Ha-Ras and was provided by Robert Weinberg (Massachusetts Institute of Technology).

AU1

Cell culture

Human HeLa cells and T47D breast cancer cells were grown in Dulbecco's modified Eagle medium (DMEM, Life Technologies, Inc., Gaithersburg, MD) containing 12.5% horse serum, 2.5% fetal calf serum, and 50 μg/ml of penicillin and streptomycin (Gibco/BRL). The MCF-12A cell line was grown in Ham's F12/DME media supplemented with 5% horse serum, 100 ng/ml cholera toxin (Gibco/BRL), 10 μg/ml insulin (Sigma, St. Louis, MO), 0.5 μg/ml hydrocortisone (Sigma), 20 ng/ml EGF (Sigma), and 50 μg/ml of penicillin and streptomycin (Gibco/BRL). All cells were grown at 37°C in 95% O_2 and 5% CO_2. Cells were passaged regularly at 70–80% confluence by harvesting in 1× PBS and 3 mM EDTA before replating in fresh media.

CAT assays

HeLa cells were grown to 60–80% confluence and then harvested in 0.05% trypsin and 0.5 mM EDTA (Gibco/BRL) and resuspended in DMEM supplemented with 12.5% horse and 2.5% fetal calf serum to a concentration of 5×10^6 cells per ml. Plasmid DNA was mixed with approximately 1×10^6 cells in a volume of 200 μl, and electroporated at 220 volts and 500 μFd using a Bio-Rad Gene Pulser. Cells were incubated for 24 h in regular growth media before harvesting for CAT assays. After 24 h, cells were harvested with 1× PBS and 3 mM EDTA, pelleted, and lysed in 0.1 M $KHPO_4$ and 0.1 M DTT. Cellular

debris was removed by centrifugation and the protein concentration in the supernatant was measured using the Bradford method. CAT assays were performed using 115 μg of protein, 20 μl of 3.3 mg/ml acetyl CoA (Boehringer Mannheim, Germany), and 10 μl of 1:10 diluted [^{14}C]-chloramphenicol (56 mCi/mmol). The volume of each reaction was normalized to 150 μl with 0.25 M Tris HCl (pH 7.8), and extracts were incubated for 1 h at 37°C before the addition of 20 μl of fresh acetyl CoA. Reactions were incubated for 1 more hour and then stopped by the addition of 800 μl of ethyl acetate. The organic phase was concentrated in a speed vacuum microcentrifuge for 30 min on medium heat (43°C), and the resulting pellet was resuspended in 25 μl ethyl acetate. The resuspended pellet was spotted onto Silica Gel 60 TLC plates (Selecto Scientific), and thin-layer chromatography was performed in 95% chloroform and 5% methanol. CAT activity was calculated based on the amount of ^{14}C that was incorporated into acetylated chloramphenicol, as quantified by phosphorimager analysis (Molecular Dynamics). Duplicate results were averaged together and the standard deviation was calculated for each set of duplicates.

AU2 AU3

Luciferase assays

HeLa cells were grown to 60–80% confluence and then trypsinized, counted, and plated in 96-well plates at a density of 4×10^4 cells per well. Cells were then transfected with 100 ng of the pA3Her2/neuLuc reporter plasmid, 1 ng of a Renilla luciferase plasmid (Promega Madison, WI) and 10, 30, 60, or 100 ng of the effector plasmids. Transfection was done according to the protocol provided with the Effectene Transfection Reagent kit (Qiagen Chatsworth, CA). Sixteen hours after transfection, the media was replaced with fresh media. Twenty hours after transfection, cells were rinsed with 1× PBS and then lysed directly on the plate with 1× Passive Lysis Buffer (Promega). Cells were allowed to incubate for 15 min in lysis buffer before the lysates were transferred to a 96-well Microlite plate (Dynex Technologies). Light units for the Her2/neuLuc and Renilla luciferase expression were read using an MLX Microtiter Plate Luminometer (Dynex Technologies) and a Promega Dual Luciferase Reporter Assay System (Promega).

AU4

Western blot analysis

HeLa cells were grown to 80% confluence and harvested, spun, and diluted as described above (see CAT assays). Cells were electroporated with 6 μg of pCGN2, pSG5, pCGN2-HA-ESX, pTL1-Elk-1, pSG5-Ets-1, and pSG5-VP16-Ets-1 at 220 volts and 500 μFd. Transfected cells were plated in 60-mm dishes and incubated for 24 h. The cells were harvested with 600 μl of 2× SDS protein load dye (Owl Separation Systems). Lysates were sheared with a 25G, 1.5″ needle several times and boiled for 5 min. Equal amounts of protein from extracts were separated on 12% SDS-polyacrylamide gels and transferred to Immobilon-P membranes (Millipore, Bedford, MA) by electrotransfer for western blot analysis. The immobilon membranes were incubated for 1 h with 5% milk and 0.2% Tween 20 in 1× PBS (blocking buffer) before being probed overnight with dilutions of either monoclonal or polyclonal HA antibody (BAbCO, Inc.) (1:1000), polyclonal ESX antibody (ABR, Inc.) (1:2500), polyclonal Ets-1 antibody (Santa Cruz Biotechnologies, Santa Cruz, CA) (1:1000), or a polyclonal Elk-1 antibody (Santa Cruz) (1:1000) in blocking buffer. Membranes were then probed with goat-antimouse-HRP or goat-antirabbit-HRP secondary antibodies (Santa Cruz Biotechnologies) in blocking buffer, for 1 h at a 1:5,000 dilution. Protein bands were then detected using enhanced chemiluminescence (ECL) (Amersham Pharmacia Biotech), according to manufacturer's directions.

AU5 AU6

MCF-12A colony formation assays

Immortalized MCF-12A cells were grown in Ham's F12/DME media containing 100 ng/ml cholera toxin (Gibco BRL), 20 ng/ml EGF (Sigma), 10 μg/ml insulin (Sigma), 5% horse serum (Gibco BRL), and 0.5 μg/ml hydrocortisone (Sigma). Cells were grown to approximately 80% confluence before being harvested with trypsin/EDTA and pelleted. Cell pellets were resuspended in complete media and approximately 4×10^5 cells were electroporated at 960 μFd and 220 volts in a volume of 200 μl with 10 μg of either empty vector pCGN2, pCGN2-HA-ESX, pCGN-HA-Ets-2, or pSV Ras. Two thousand cells were plated in complete media in triplicate in 60-mm tissue culture dishes and grown in 95% O_2 and 5% CO_2 at 37°C. Media was changed every 2–3 days for the duration of the incubation. On the 13th day of incubation, colonies were rinsed with 1× PBS and fixed with a graded methanol series of 50, 70, 90, 95, and 100% methanol for 5 min each. Fixed cells were then stained for 5 min with Wright's stain (Sigma), followed by a 10-min incubation in a 1:10 dilution of Giemsa stain (Sigma). Colonies were rinsed several times with H_2O to reduce background stain, and then photographed and counted manually based on a colony size that was greater than 1 mm in diameter.

T47D colony formation assays

Human T47D breast cancer cells were harvested at approximately 70–80% confluence in 0.05% trypsin and 0.5 mM EDTA. Cells were spun and resuspended in DMEM containing 12.5% horse serum and 2.5% fetal calf serum to a concentration of approximately 1×10^6 cells per 200 μl volume. Cells were cotransfected in a 200 μl volume with 2 μg of a plasmid containing green fluorescent protein (EGFP, Clontech, Palo Alto, CA) and 20 μg of plasmids encoding for either antisense ESX (pCGN2-HA-anti-ESX), dominant-negative ESX (pCDNA3.1-HA-ESC DBD), or empty vector (pCGN2) by electroporation and plated in 60-mm plates. Twenty-four hours posttransfection, cells were harvested with 1 × PBS and 3 mM EDTA and were spun down before resuspending in media for flow-cytometric analysis. Flow-cytometric analysis was performed in sterile conditions to select for green fluorescent cells with a FACScan fluorescent-activated cell analyzer at the University of Colorado Health Sciences Center Flow-Cytometric Core Facility. Two thousand sorted, green-fluorescent cells were seeded in 60-mm dishes in 3 ml of complete growth media containing 12.5% horse serum and 2.5% fetal calf serum. After cells had adhered to the plate, media was removed and fresh media with 0.1, 1, or 5% serum was added to the cells. Cells were allowed to incubate for 13 days, during which the media was replaced every 2 days. On day 13, plates were rinsed with 1 × PBS and then fixed and stained using Crystal Violet (Sigma). Colonies were counted manually.

RESULTS

Expression of HA-ESX

In vitro transcription and translation reactions were performed to characterize ESX protein expression and migration on SDS-polyacrylamide gels. Translation products labeled with S^{35}-methionine were separated by electrophoresis on a 10% polyacrylamide gel, blotted onto a nitrocellulose membrane, and detected by autoradiography (Fig. 2). As a negative control, the reticulocyte lysate reaction was carried out in duplicate in the absence of input DNA and no specific translation product was detected (Fig. 2, lanes 1 and 2). As a positive control, the reticulocyte lysate assay was performed in duplicate with chicken Ets-1 DNA, and the predicted 68-kDa protein product was consistently noted as a doublet (Fig. 2, lanes 3 and 4). *In vitro* transcription and translation of pCDNA3.1-ESX plasmid, also performed in duplicate, resulted in a protein migrating at 47 kDa (Fig. 2, lanes 5 and 6). Contrary to theoretical size calculations, which predict a size of 42 kDa for ESX protein, we determined that ESX migrated at 47 kDa by plotting the relative migration (Rf) of the protein versus the log of the molecular weight. This was done by analyzing gels of various polyacrylamide percentages to verify the 47-kDa migration pattern of ESX (data not shown). To further characterize ESX expression *in vivo*, a plasmid construct expressing an HA-tagged version of ESX protein (pCGN2-HA-ESX) was transiently transfected into HeLa cells. ESX was immunoprecipitated from transfected HeLa cell lysates using a monoclonal anti-HA antibody (data not shown). HeLa cells transfected with the pCGN2-HA-ESX produced a 48-kDa protein (data not shown), which is consistent with the migration of 47 kDa for ESX plus the 1 kDa contributed by the HA tag.

Transcriptional potency of HA-ESX

Having shown that HA-ESX is expressed after transient transfection, we next sought to determine its relative transcription potencies. We used the 8xpal-pBLCAT as a reporter construct, because it contains eight copies of an Ets binding site derived from the rat stromelysin promoter (Wasylyk *et al.*, 1991). HeLa cells were transfected in duplicate with 4 μg of the empty vector control, pCGN2, and only minimal amounts of CAT activity were detected (Fig. 3A, lanes 1 and 2, and Fig. 3B). Duplicate transient transfection with increasing amounts of pCGN2-HA-ESX DNA resulted in a dose-dependent increase in 8xpal-pBLCAT transcription activity, with 1, 2 and 4 μg of pCGN2-HA-ESX DNA resulting in 3.2, 6.2, and 14.9% conversion to acetylated chloramphenicol, respectively, reflecting CAT activity (Fig. 3A, lanes 3–8, and Fig. 3B). Additionally, duplicate transfection of 2 μg of either pCGN2-HA-Ets-2 or of pSVRas, as positive controls, resulted in 7.8 and 10.1% conversion to acetylated chloramphenicol, respectively (Fig. 3A, lanes 9–12, and Fig. 3B).

Differential activation of metalloproteinase promoters by ESX

Matrix metalloproteinase genes have been shown to be key targets of Ets proteins, and it has been suggested that the Ets-mediated induction of these genes contributes to the invasive and angiogenic phenotypes of malignant cells (Gilles *et al.*, 1997; Watabe *et al.*, 1998; Oda *et al.*, 1999). Although HA-ESX was capable of activating the 8xpal pBLCAT reporter construct, it should be noted that this is an artificial promoter construct containing eight copies of the stromelysin Ets binding site (EBS) fused upstream of a minimal TK promoter (Wasy-

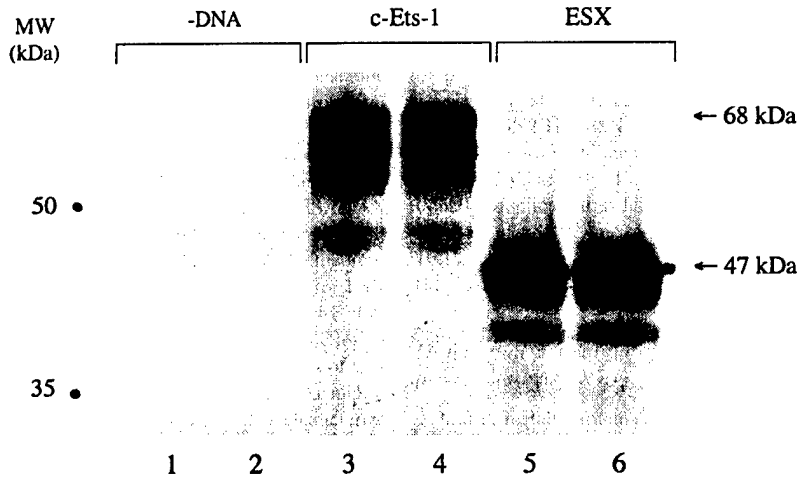

FIG. 2. *In vitro* transcription and translation of HA-ESX. The negative controls represent *in vitro* transcription and translation reactions without any input DNA (lanes 1 and 2). One microgram of chicken Ets-1 was used as a positive control (lanes 3 and 4) and 1 μg of [pCDNA3.1-ESX was used for the *in vitro* transcription and translation of ESX (lanes 5 and 6). Radiolabeled translation products were separated by SDS-PAGE. The dots denote pen-marks corresponding to the 50- and 35-kDa size markers, and the arrow denotes ESX protein, the size of which was determined by plotting the relative migration of ESX versus the log molecular weight. Figure depicts representative experiment performed in triplicate.

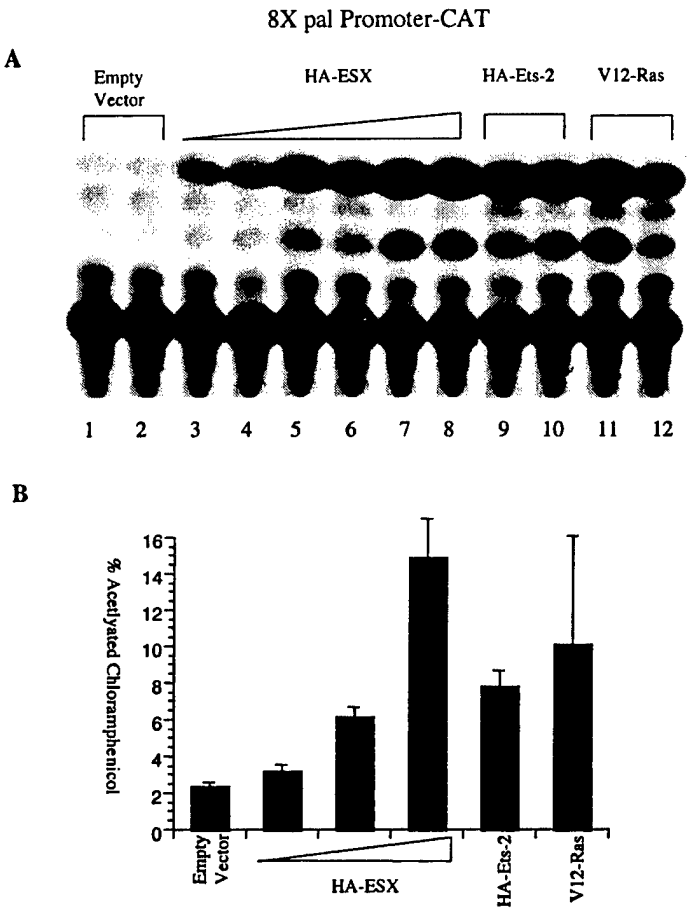

FIG. 3. Activation of the 8xpal promoter by HA-ESX, HA-Ets-2, and V12-Ras. (**A**) CAT Assay. HeLa cells were cotransfected with the reporter construct 8xpal/pBLCAT and various doses of effector plasmids. pCGN2 vector was used for the vector control (lanes 1–2). Lanes 3–8 show CAT activity in response to three increasing doses of HA-ESX, 1, 2, and 4 μg, respectively (performed in duplicate). Two positive control effectors were used, including 2 μg of HA-Ets-2 (lanes 9–10) and 2 μg of V12-Ras (lanes 11–12). (**B**) Quantitation of percent acetylated chloramphenicol generated by the 8xpal promoter in response to HA-ESX, HA-Ets-2, and V12-Ras. The amount of CAT activity in percent was calculated by dividing the amount of acetylated chloramphenicol by the amount of total chloramphenicol in the duplicate samples, and the mean is shown ±SD, as described in Materials and Methods. Autoradiograph depicts representative performed in triplicate.

lyk *et al.*, 1991). Therefore, we next determined the ability of HA-ESX to activate the EBS in the context of the authentic stromelysin promoter, and whether these Ets factors could activate other metalloproteinase promoters. Figure 4A (lanes 1 and 2) and Figure 4B, show that the activity of the rat −1100 stromelysin promoter transfected into HeLa cells is minimally detectable (2.5% conversion to acetylated chloramphenicol). Surprisingly, pCGN2-HA-ESX and pCGN2-HA-Ets-2 (10 μg each) failed to activate the −1100 rat stromelysin promoter (Fig. 4A, lanes 3–6, and Fig. 4B). Furthermore, doses of pCGN2-HA-ESX ranging from 0.1 to 20 μg failed to produce CAT activity at any dose, suggesting that the lack of stromelysin promoter activity was not due to squelching effects or to insufficient expression of this construct (data not shown). By contrast, 10 μg of pSV Ras and pSG5c-Ets-1 caused robust activation of the −1100 rat stromelysin promoter (Fig. 4A, lanes 7–10, and Fig. 4B), showing that this reporter is functional. Moreover, this lack of transcriptional effect of HA-ESX, and HA-Ets-2 is not due to the presence of a TGFβ inhibitory element (TIE) on the rat −1100 stromelysin promoter, because similar analysis of a truncated rat stromelysin promoter (−550-CAT) lacking the TIE (TGF-beta inhibitory element) was used to determine potential changes in activation by HA-ESX, HA-Ets-2, c-Ets-1, and V12-Ras on a promoter without the TIE. Although V12-Ras activation of the −550 stromelysin promoter appeared to be less than that of the −1100 promoter, no other significant differences were noted in the activation pattern of the shortened rat stromelysin promoter (data not shown).

To further determine the role of ESX in metalloproteinase gene activation, we chose to investigate whether ESX could ac-

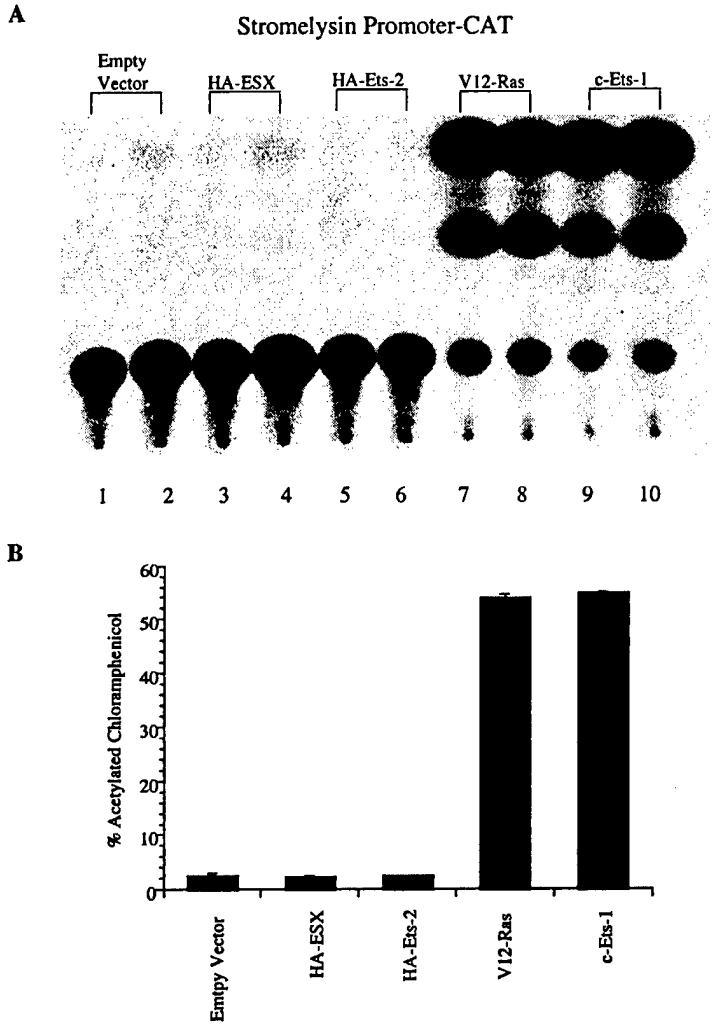

FIG. 4. Activation of the stromelysin promoter by V12-Ras and c-Ets-1 but not HA-ESX or HA-Ets-2. (**A**) CAT Assay. HeLa cells were transfected with 5 μg of a stromelysin–CAT construct containing −1100/+8 of the rat stromelysin promoter together with 10 μg of empty vector (lanes 1–2), HA-ESX (lanes 3–4), HA-Ets-2 (lanes 5–6), V12-Ras (lanes 7–8), or c-Ets-1 (lanes 9–10). (**B**) Quantitation of CAT activity produced by the −1100/+8 stromelysin–CAT construct in response to various effector plasmids. The % acetylated chloramphenicol was calculated as described in Figure 3B. Autoradiograph depicts representative performed in triplicate.

tivate the collagenase promoter, which also contains an ETS binding site. Here, we show that HA-ESX and HA-Ets-2 were capable of activating the −517 to +63 region of the human collagenase promoter (Fig. 5). As was the case with the stromelysin promoter, the human collagenase promoter had no detectable basal activity when transfected into HeLa cells (Fig. 5A, lanes 1 and 2, and Fig. 5B). Moreover, transfection of empty vector had no effect on basal collagenase promoter activity, whereas HA-ESX resulted in a dose-dependent and strong activation of this reporter. As shown in Figure 5A, lanes 3–8, and quantitated in Figure 5B, HA-ESX resulted in 2.2, 13.5, and 44.5% conversion to acetylated chloramphenicol at 1, 5, and 10 μg of DNA input, respectively. The two positive controls, human HA-Ets-2 (10 μg) and V12-Ras (10 μg), mediated robust activation of the collagenase promoter, resulting in 28.6 and 33.2% conversion to acetylated chloramphenicol, respectively (Fig. 5A, lanes 9–12, and Fig. 5B).

F5

Response of the Her2/neu promoter to nine distinct Ets factor constructs

Overexpression of the Her2/neu proto-oncogene is found in about 30% of human breast cancers, and this overexpression is thought to contribute to mammary tumorigenesis (Liu *et al.*, 1992). Furthermore, the proximal region of the Her2/neu promoter contains a functional Ets binding site immediately up-

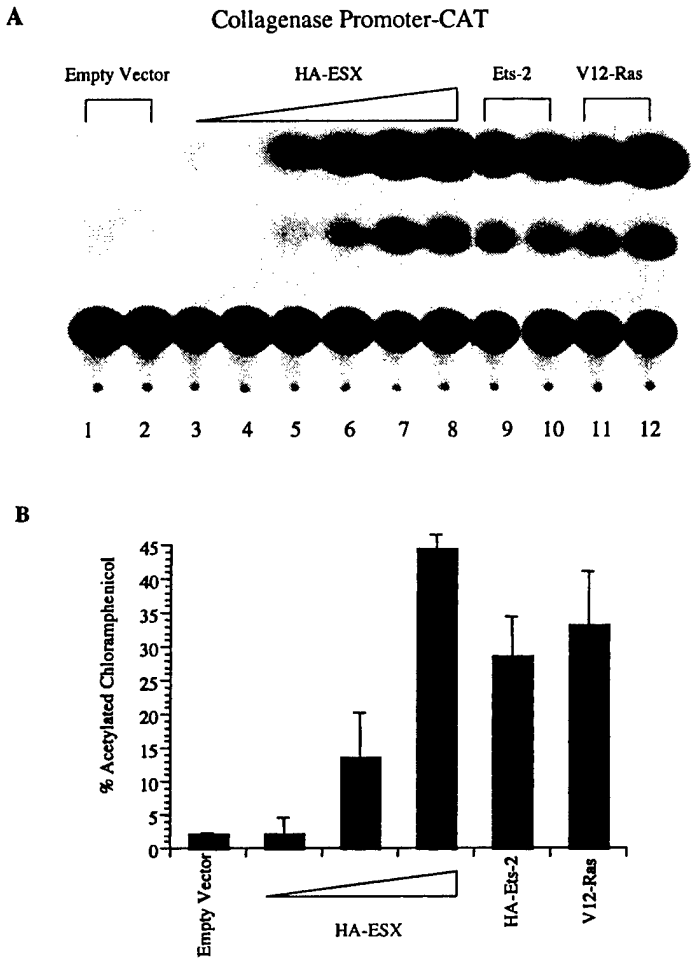

FIG. 5. Activation of the collagenase promoter by HA-ESX and HA-Ets-2 in HeLa cells. (**A**) Cat Assay. Five micrograms of the human collagenase promoter (−517/+63) fused to a CAT reporter gene was transfected into HeLa cells with 1, 5, or 10 μg of HA-ESX. Ten micrograms of human HA-Ets-2 and V12-Ras served as positive controls for human collagenase promoter activity. (**B**) Quantitation of CAT activity produced by the −517 collagenase–CAT construct in response to various effector plasmids, as in Figure 3B. Because the autoradiograph in (**A**) was exposed beyond the liner range in an attempt to unmask HA-ESX and HA-Ets-2 activity, the CAT activities do not appear to match with those shown in (**B**), which were obtained by phosphorimager analysis, which maintains linearity. Autoradiograph depicts representative performed in triplicate.

stream of the TATA-box, at position −26, which has been shown to respond to cotransfected PEA3 (Benz *et al.*, 1997; Xing *et al.*, 2000) and ESX (Scott *et al.*, 1994; Chang *et al.*, 1997) in transient transfection reporter assays. Because multiple Ets factors have been shown to be expressed in breast cancer cell lines (Trimble *et al.*, 1993; Scott *et al.*, 1994; Baert *et al.*, 1997; Chang *et al.*, 1997; Gilles *et al.*, 1997; Watabe *et al.*, 1998), the precise identity of the specific Ets factor that activates the Her2/neu promoter *in vivo* remains unknown. Thus, we chose to test the ability of increasing doses of constructs encoding nine distinct Ets family members to activate the Her2/neu promoter, to determine the relative transcription potencies of these Ets factors on the Her2/neu promoter. The −497 to +30 region of the human Her2/neu promoter region was cloned into a luciferase reporter plasmid (pA3Luc) and the effects of Elk-1, ER-81, c-Ets-1, VP16-Ets-1, NET, GABP, EHF, HA-ESX, and HA-Ets-2 on the Her2/neu promoter was examined (Fig. 6). The results were grouped according to the mammalian expression vector used to drive these various Ets factors. Figure 6A shows those driven by an SV40 promoter-based vector (Elk-1, ER81, Ets-1, and VP16-Ets-1), and Figure 6B shows those driven by CMV promoter-based vectors (NET, GABP, EHF, HA-ESX, and HA-Ets-2).

F6

For the SV40 promoter-driven Ets factors, pSG5 was used as the empty vector (Wasylyk *et al.*, 1991). Increasing doses of an empty pSG5 vector had minimal effects on the activity of the Her2/neu promoter, whereas Elk-1 resulted in a strong dose-dependent reduction in promoter activity (Fig. 6A). In contrast,

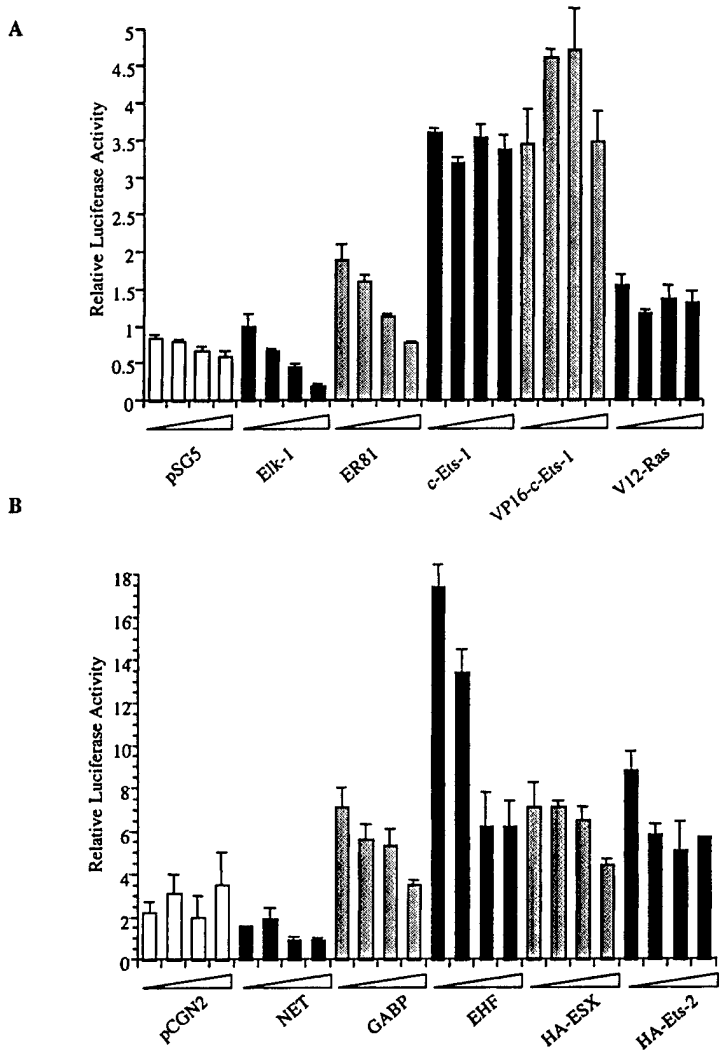

FIG. 6. Transcription potency of various Ets factor constructs on the human Her2/neu promoter. (**A**) The transcription effects of pSG5-driven Elk-1, ER-81, c-Ets-1, VP16-c-Ets-1, and V12-Ras on the Human Her2/neu promoter. In a 96-well plate, doses of 10, 30, 60, and 100 ng of effector DNA were transfected into HeLa cells together with 100 ng of Her2/neu-pA3Luc reporter plasmid. Empty vector pSG5, containing the SV40 promoter, served as the negative control for these effectors, because the SV40 promoter is common to all of these constructs. (**B**) The transcription effects of pCMV-driven NET, GABP, EHF, HA-ESX, and HA-Ets-2 on the Her2/neu promoter. In a 96-well plate, doses of 10, 30, 60, and 100 ng of effector DNA were transfected into HeLa cells together with 100 ng of Her2/neu-pA3Luc reporter plasmid. Empty vector pCGN2, containing the CMV promoter, served as the negative control for these effectors, Because the CMV promoter is common to all of these constructs. Activation of reporter plasmids by the various transcription factors was determined by measuring normalized luciferase activity, which was then calculated as fold activity of the empty vector control, as detailed in Materials and Methods.

ER81, Ets-1, and VP16-Ets-1 all resulted in activation of the Her2/neu promoter. Of note, ER81 resulted in a modest ~twofold response of the Her2/neu promoter at the lowest DNA input, and this response was completely abrogated with increasing doses of ER81 input DNA (Fig. 6A). All doses of c-Ets-1 and VP16-Ets-1 activated the Her2/neu promoter nearly equally, with c-Ets-1 mediating an average ~5.5-fold response and VP16-Ets-1 mediating an average ~sixfold response (Fig. 6A). Finally, V12-Ras produced about a twofold activation of the Her2/neu promoter at all doses tested (Fig. 6A).

For the CMV promoter-driven Ets factors, pCGN2 (Gordon *et al.*, 1997; Bradford *et al.*, 2000) was used as the CMV promoter-containing, empty vector control. As shown in Figure 6B, increasing doses of pCGN2 had no significant effects on the activity of the Her2/neu promoter. By contrast, NET, a repressor Ets transcription factor, inhibited Her2/neu promoter activ-

ity by approximately 50%, compared to vector-only controls (Fig. 6B). GABP (containing equal amounts of GABPα and GABPβ) resulted in a ~3.5-fold response at the lowest DNA dose, and this effect was eliminated completely with increasing doses of input DNA. EHF mediated an ~8.5-fold response of the Her2/neu promoter, which was also reduced in a DNA dose-dependent manner. However, EHF maintained a ~threefold effect at the highest DNA dose (Fig. 6B). HA-ESX resulted in a ~3.5-fold response at the first three doses of input effector DNA, and this response was reduced slightly to a ~twofold effect at the highest input DNA. Finally, HA-Ets-2 mediated a fourfold response at the lowest input DNA, and then stabilized to a 2.5-fold response at the subsequent three higher input DNA doses (Fig. 6B). These data show that the Her2/neu promoter responds differentially to distinct Ets family members. Specifically, the HER2/neu promoter revealed three patterns of gene activation by these constructs encoding nine distinct Ets factors: (1) no effect or repressed promoter activity (Elk-1 and NET); (2) intermediate activity (ER81, GABP, HA-ESX, and HA-Ets-2); and, (3) maximal activity (Ets-1, VP-16-Ets-1, and EHF).

Expression of various transfected Ets factor proteins

One possible explanation for the differential activation of the Her2/neu promoter by the various Ets factors is that there is a marked differential expression of these Ets constructs in HeLa cells, producing a significantly variable amount of transfected Ets proteins. To address this point, we performed Western blot analysis of select Ets proteins after Ets expression vector transfection into HeLa cells. The Her2/neu transactivation studies described above were performed in a microscale using ~10^4 cells and nanogram amounts of expression vector DNA in a 96-well format, which would not produce sufficient Ets proteins to be detectable by Western blot analysis. To circumvent this issue, we performed large-scale transfections of several of these Ets expression vectors, essentially using the same cell number and DNA dose range as used in Figures 3–5. Figure 7A and B shows that, in the pSG5 group, the level of expression of recombinant Elk-1, Ets-1, and VP16-Ets-1, normalized for actin as a loading control, was easily detectable. Similarly, Figure 7C and D show that, in the pCGN group, the level of expression of recombinant HA-ESX and HA-Ets-2 were also robustly expressed. Taken together, these data validate that the significant differences seen in Her2/neu promoter activity were not attributable to a lack of expression of select Ets effector proteins, but rather were due to intrinsic differences in transcription potency of these various Ets factors on the Her2/neu promoter.

ESX positively modulates colony formation in MCF-12A cells

Having established the ability of HA-ESX to transcriptionally activate promoters involved in tumorigenesis, we chose to determine whether ESX could function as a cell survival and growth-promoting factor. To accomplish this, the immortalized but nontransformed human breast epithelial cell line, MCF-12A, which does not express ESX (data not shown), was used

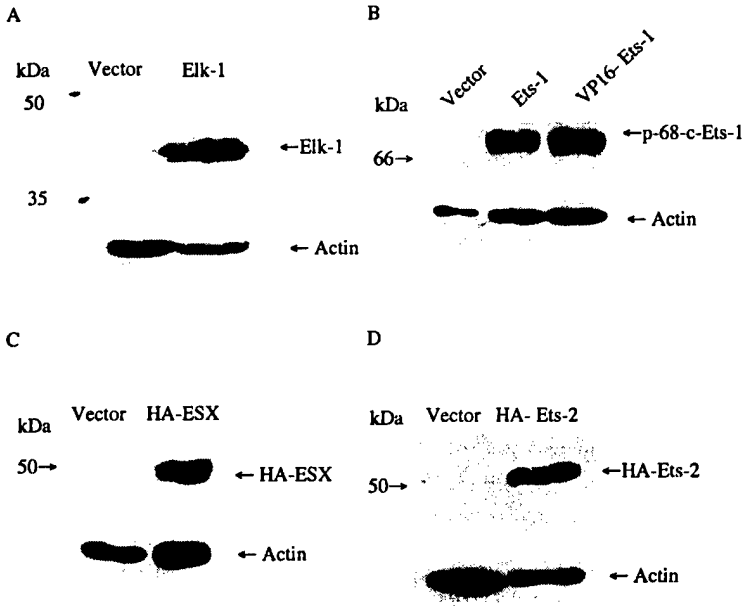

FIG. 7. Western blot analysis of transfected Elk-1, c-Ets-1, VP16-c-Ets-1, HA-ESX, and HA-Ets-2 in HeLa cells. HeLa cells were transfected by electroporation with (A) 6 μg of pSG5 or pTL-Elk-1; (B) 6 μg of pSG5, pSG5-c-Ets-1, or VP16-cEts-1; (C) 6 μg of pCGN2 or pCGN2-HA-ESX; and (D) 6 μg of pCGN2 or pcGN2-HA-Ets-2. After a 24-h incubation, cells were harvested and lysed, and cell extracts were analysed by Western blot analysis with the appropriate anti-Ets or anti-HA antibody, as described in Materials and Methods. Representative Western blots are shown. Experiment performed in triplicate.

to evaluate the growth-promoting properties of HA-ESX, HA-Ets-2, and V12-Ras in colony formation assays. MCF-12A cells were transfected with the empty vector (pCGN2) or the various Ets constructs, plated at a low density in complete Ham's F12/DME media and cultured for 13 days prior to staining the colonies. Colonies were measured, and all colonies greater than 1 mm in diameter were counted. Figure 8 shows that transfection with the negative pCGN2 control resulted in a minimal number of colonies, averaging six colonies/plate, whereas the positive control, oncogenic V12-Ras, resulted in a higher number (~32 colonies/plate) of colonies over 1 mm in diameter (Fig. 8 and Table 1). The HA-ESX resulted in ~17 and colonies/plate which is about threefold greater than the vector-only results (Fig. 8 and Table 1). Finally, HA-Ets-2 revealed an ability to form colonies in MCF-12A cells, resulting in ~23 colonies/plate, which is similar to HA-ESX (Fig. 8 and Table 1); however, HA-Ets-2 appeared competent to efficiently induce many colonies smaller than 1 mm in diameter.

F8 T1

Antisense ESX and dominant-negative ESX suppress colony formation of T47D human breast cancer cells

The ability of HA-ESX to induce colony formation in ESX-negative MCF-12A cells suggested to us that ESX might be required for mammary cell survival and growth. To test this possibility, we chose to determine the role of endogenous ESX in colony formation in transformed T47D human breast cancer cells, because this cell line expresses easily detectable levels of ESX and HER2/neu protein (data not shown). To this end, we transfected T47D cells with pGFP and either HA-antisense-ESX or a dominant-negative HA-ESX DBD (containing only the AT-hook and DNA-binding domains) in a 1:10 ratio and selected for the transfected population by FACS for GFP fluorescence. This enriched population of transfected cells was then plated in various concentrations of serum (0.1, 1, and 5%), and colony formation was recorded (Fig. 9) and quantitated (Table 2) 13 days later, as described in the Materials and Methods sec-

F9 T2

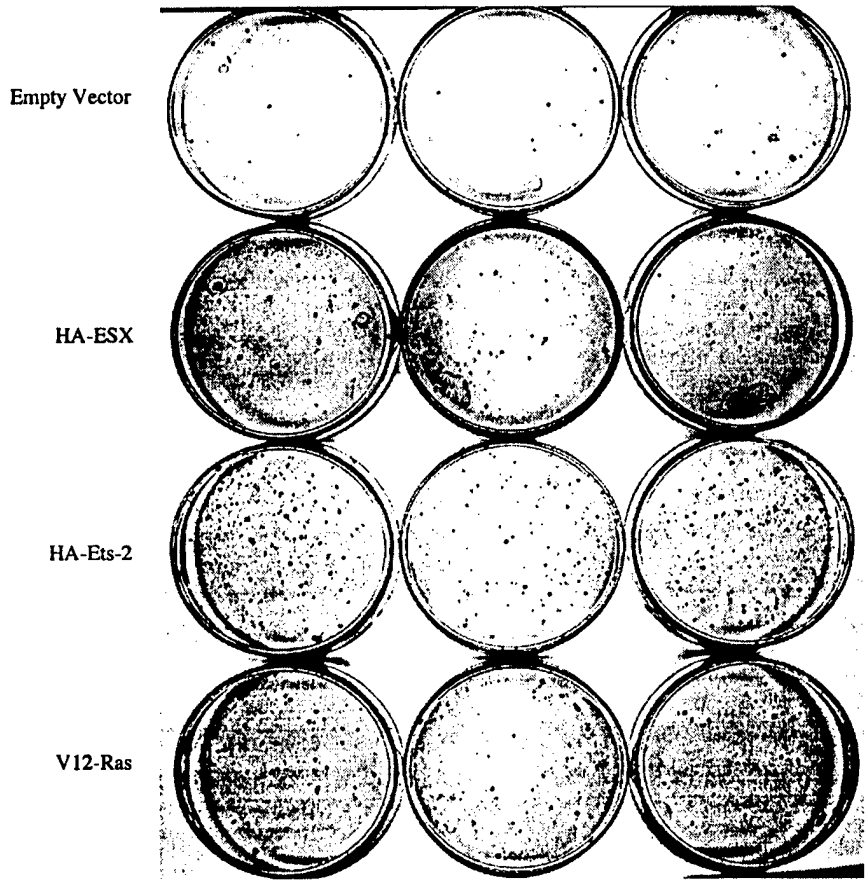

FIG. 8. HA-ESX and HA-Ets-2 induce colony formation of nontransformed MCF-12A breast cells. Human MCF-12A mammary cells were transfected by electroporation with 10 μg of pCGN2 (empty vector), pCGN2-HA-ESX (HA-ESX), pCGN-HA-Ets-2 (HA-Ets-2), or pSV-Ras (V12-Ras), and 1×10^3 electroporated cells were plated per dish, in triplicate. Plates were incubated for 13 days and media was changed every 2–3 days throughout the 13-day incubation. Following this incubation, colonies were fixed and stained with Wrights/Giemsa as described in Materials and Methods. Representative plates are depicted in triplicate, and experiment was performed in triplicate.

TABLE 1. INDUCTION OF MCF-12A COLONY FORMATION BY ETS FACTORS[a]

Empty vector	*HA-ESX*	*HA-Ets-2*	*V12-Ras*
6 (±3)	17 (±6)	23 (±17)	32 (±8)

[a]Triplicate results shown in Figure 8 were counted (colonies ≥1 mm) and the average number of colonies per plate (± SD) are tabulated.

tion. As shown in Figure 9, T47D cells transfected with empty vector control resulted in numerous cell colonies, ranging from 301–326, at all serum concentrations (Table 2). Indeed, the effect of increasing serum concentration primarily affected colony size in these empty vector controls (Fig. 9). By contrast, T47D cells transfected with antisense ESX resulted in a significant reduction in colony formation, resulting in 67, 82, 126 colonies at 0.1, 1, and 5% FCS, respectively. Compared to the empty vector results at each equivalent serum concentration, these numbers represent 22, 28, and 39% colony-forming efficiency, respectively (Table 2). Finally, T47D cells transfected with a truncated dominant-negative version of ESX reveals similar reductions in colony formation, resulting in 52, 67, and 146 foci at 0.1, 1, and 5% FCS, respectively (Fig. 9 and Table 2). These data represent 17, 22, and 45% colony-forming efficiency at 0.1, 1, and 5% FCS, respectively, compared to vector controls (Fig. 9 and Table 2). Similar studies performed by transducing T47D cells with an adenovirus construct expressing either GFP alone or GFP plus antisense ESX revealed the same inhibitory effect of antisense ESX on T47D cell survival (data not shown).

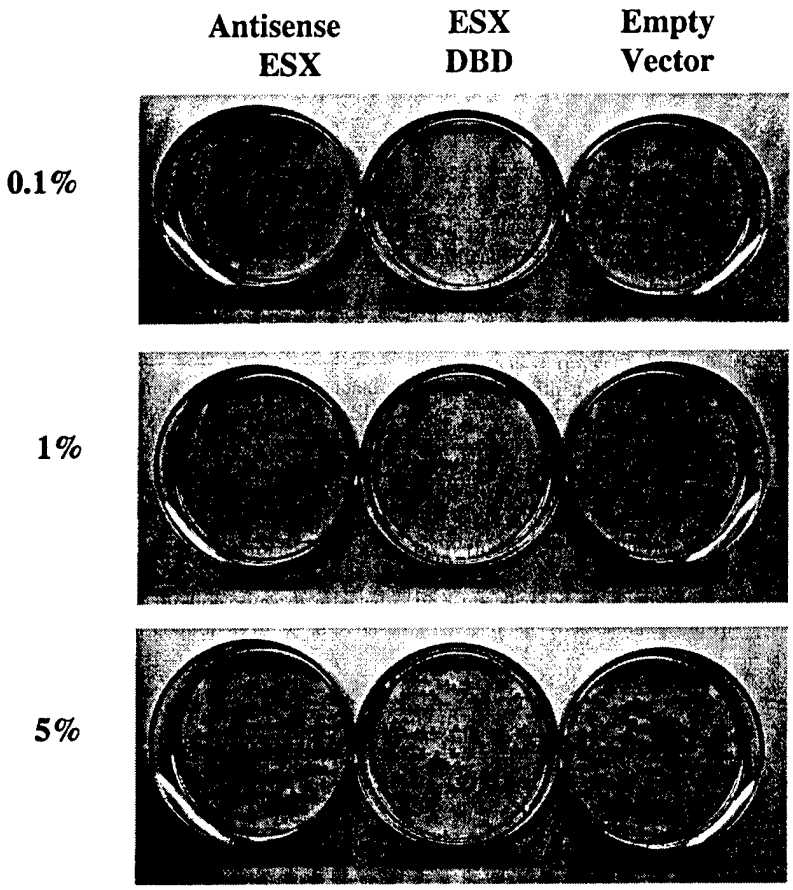

FIG. 9. Antisense-ESX and HA-ESX DBD inhibit colony formation of transformed T47D breast cancer cells. T47D cells were cotransfected with a plasmid encoding green fluorescent protein (GFP) and either plasmids encoding inhibitory ESX effectors (antisense HA-ESX or dominant-negative HA-ESX DBD) or empty vector (shown at the top). Transfected cells were sorted according to green fluorescence and 2,000 sorted cells were plated in 60-mm dishes, in three different concentrations of fetal calf serum, 0.1, 1, or 5% (shown on the left), and then allowed to incubate for 13 days. Colonies were fixed and stained with crystal violet as described in Materials and Methods. Representative plates are depicted in triplicate, and experiment was performed in triplicate.

TABLE 2. INHIBITION OF T47D COLONY FORMATION BY INHIBITORY ESX CONSTRUCTS[a]

% FCS	HA-antisense-ESX	HA-ESX DBD	Empty vector
0.1	67 (22%)[b]	52 (17%)	303
1	82 (28%)	67 (22%)	301
5	126 (39%)	146 (45%)	326

[a]Triplicate results shown in Figure 9 were counted and the average number of colonies per plate is tabulated.
[b]Numbers in parenthesis represent the % of total colonies formed by empty vector.

DISCUSSION

Although a number of studies have implicated several Ets family members in mammary tumorigenesis, the precise role of any specific Ets factor in breast cancer remains unknown. In this study, we show that the epithelial-specific Ets family member, ESX, is expressed from mammalian expression vectors resulting in a protein of about ~47 kDa that is able to differentially activate several promoters, including the collagenase promoter, and to mediate colony formation of MCF-12A nontransformed mammary cells. In addition, antisense and dominant-negative ESX reduces clonagenic growth of T47D transformed breast cells. Thus, we have shown by several different approaches that ESX modulates the expression of breast cancer-associated genes and promotes breast cell survival and/or growth. These results are significant in that they provide evidence of the critical requirement of ESX for breast cell survival and/or growth.

ESX is expressed as a 47 kDa protein in vitro *and* in vivo

Two distinct cDNA clones for human ESX have been isolated, differing in length by 69 nucleotides (Oettgen *et al.*, 1997). The predominant, larger isoform apparently results from an alternative splice site that is about 69 nucleotides 5′ of the exon 3 splice acceptor site, resulting in an ESX containing an extra 69 nucleotides in exon 3 (Oettgen *et al.*, 1997). The EXS protein derived from the larger ESX mRNA encodes for a protein of 371 amino acids that is predicted to migrate at 41.4 kDa (Oettgen *et al.*, 1997). In contrast, the smaller mRNA, devoid of the 69 nucleotides, is predicted to migrate at 39.3 kDa (Oettgen *et al.*, 1997). Here, we used the larger isoform of human ESX and showed that the protein produced by this construct migrates at 47 kDa, both *in vitro* (Fig. 2) and *in vivo* (Fig. 7). Moreover, recombinant GST-ESX migrated at ~74 kDa, and allowing for the 27 kDa of GST reveals that bacterially expressed ESX also migrates at 47 kDa (data not shown). These data contrast with those of Chang *et al.* (1999), who used a polyclonal antibody to the carboxy-terminal end of ESX to demonstrate that endogenous ESX expressed in several breast cancer cell lines (ZR75-1, MDA-468, and MDA-231) migrated as a 42 kDa protein band. Of note, this latter report did not show protein size standards, and instead only showed the ESX bands in isolation (Chang *et al.*, 1999). These minor differences in ESX protein migration might be due to slight experimental differences.

Differential transcription potency of ESX on various Ets-target promoters

In this report, we show that ESX differentially activates various promoters, each of which contains a functional Ets binding site (EBS). Thus, ESX efficiently activated the 8Xpal, collagenase, and Her2/neu promoters, but failed to activate the stromelysin promoter (Figs. 3–6). Of note, the single EBS within the stromelysin promoter is the same as the EBS that is multimerized as eight copies in the 8xpal promoter (ATTTGGATGGAAGCAATTAT), yet ESX failed to activate the former, but clearly activated the latter. These data show that a single EBS of the type contained within the stromelysin promoter is insufficient to mediate ESX activity. By contrast, the single EBS contained within the collagenase or Her2/neu promoters appears to be sufficient to allow ESX-mediated promoter activation. The EBS within the collagenase promoter is ACTAGGAAGTGGAAA at position −85 (Pendas *et al.*, 1997) and the EBS within the Her2/neu promoter is TGCTTGAGGAAGTATAA located at position −26 (Scott *et al.*, 1994). In addition, Choi *et al.* (1998), examined the ability of various Ets binding sites contained in seven different promoters, including TGFβ RII, Tra, IL-2Ra, PEA3, HTLV-1, CD18, and HIV2, to bind ESX by gel shift analysis, and to be activated by ESX in transient cotransfection assays. These studies identified the PEA3 (CGAGCAGGAAATGGG), TRα (AGCCACATCCTGTGGAA), TGFβ RII (GGAAACAGGAAACTCCT), and HTLV-1 (CATGGGGAGGAAATGGG) Ets binding sites as binding to ESX in gel shifts studies, and as being activated two- to fourfold by cotransfected ESX (Choi *et al.*, 1998). In a separate study, the relative binding affinity of ESX for Ets binding sites derived from 10 different epidermis-selective genes was performed and, using the resultant data, a consensus ESX binding sequence was defined as: 5′-(A/G/T)N(C/G/a)(A/c)GGA(A/t)(G/a)(T/a/c)(A/G/c)(N/t)-3′ (Oettgen *et al.*, 1999). Although the ESX binding site sequence prefers the nucleotide A immediately upstream of the core GGA and most other Ets factors prefer a C at that site (Graham and Gilman, 1991; Graves and Petersen, 1998); nevertheless, the ESX site is quite degenerate. In this regard, a comparison of the Ets binding sites noted above for stromelysin, collagenase, and Her2/neu show that the sites from the latter two ESX-stimulated genes match the consensus ESX sequence, whereas the nonresponsive stomelysin site contains a T just upstream of the core GGA and a C three bases downstream of the core sequence. It is likely that these two changes account for the reduced ability of ESX to stimulate the stromelysin promoter. However, the negative

effects of these two nonconsensus bases are overcome if this stromelysin site is present in multiple copies, as in 8Xpal.

Differential activation of the HER2/neu promoter by nine distinct Ets constructs

As noted above, the HER2/neu promoter has been shown to contain a critical EBS at position −26 (Chang *et al.*, 1997). The Ets factors PEA3 and ESX have been shown to be overexpressed in Her2/neu positive breast cancer cells, and to bind to the −26 site and to activate Her2/neu promoter-reporter constructs in co-transfection assays (Scott *et al.*, 1994; Benz *et al.*, 1997). However, the identity of the endogenous Ets factor that actually regulates Her2/neu promoter activity via the −26 site *in vivo* remains unknown. Here we show that, in fact, several Ets factors stimulated the her2/neu promoter (Fig. 6). Of note, several Ets factors have been shown to be expressed in mammary cells, including members of the PEA3 subfamily (PEA3, ER81, and ERM), GABP, Ets-1, Ets-2, ESX, and Elk (Shepherd and Hassell, 2000) and of these Ets factors, both PEA3 and ESX have been reported to activate the Her2/neu proximal promoter in co-transfection assays (Scott *et al.*, 1994; Benz *et al.*, 1997; Chang *et al.*, 1997; Xing *et al.*, 2000). In this study, three patterns of Her2/neu promoter activation by Ets factors were demonstrated: (1) no effect or repressed promoter activity (Elk-1 and NET); (2) intermediate activity (ER81, GABP, HA-ESX, and HA-Ets-2); and, (3) maximal activity (Ets-1, VP-16-Ets-1, and EHF). These different patterns of Her2/neu gene promoter activation by the various Ets factors are unlikely to be due to very low levels of Ets protein expression, as documented in Figure 7. Taken together, these data show that indeed multiple Ets factors, including ER81, GABP, Ets-1, Ets-2, EHF, and ESX, are capable of *trans*-activating the Her2/neu promoter. It is noteworthy that heregulin has been shown to induce PEA3 and ESX expression, which in turn, can activate the Her2/neu promoter, suggesting that a positive feedback loop between Her2/neu and specific Ets factors may exist in Her2/neu positive breast cancer cells (Benz *et al.*, 1997; Neve *et al.*, 1998).

ESX and Ets-2 promote MCF-12A colony formation, whereas antisense and dominant-negative ESX inhibit T47D colony formation

The proto-oncogenes *c-Ets-1* and *c-Ets-2* are able to transform NIH 3T3 cells, but at a much reduced efficiency (less than 50-fold) compared to the *gag-myb-ets* oncogene (Seth and Papa, 1990). Foos et al. (1998) have reported that the role of Ets-2 in cellular transformation may be quite complex, because overexpression of full-length Ets-2, a VP16-Ets-2 fusion or the Ets-2 DBD, reversed the Ras-mediated transformation of NIH 3T3 cells (Foos *et al.*, 1998). By contrast, the Ets-2 TAD failed to fully reverse the transformed phenotype (Foos *et al.*, 1998). Taken together, these data would suggest that Ets-1 and Ets-2 are weak transforming agents, and that their mechanisms of transformation may be complex.

As noted in the Introduction, the use of dominant-negative Ets-2, which encodes for only the Ets-2 DBD, has provided the most substantial data implicating Ets proteins in mammary cell tumorigenesis (Delannoy-Courdent *et al.*, 1998; Sapi *et al.*, 1998). Specifically, dn-Ets-2 has been shown to totally block the anchorage-independent growth and cellular invasiveness of NmuMG, MMT, and BT20 breast carcinoma cells (Delannoy-Courdent *et al.*, 1998; Sapi *et al.*, 1998). Moreover, the size of mammary tumors induced by a polyoma virus middle T antigen (PyMT) transgene were reduced in half in mice that were also heterozygous for a *c-Ets-2* loss-of-function mutation (Neznanov *et al.*, 1999). Dominant-negative Ets-2, and to a lesser extent dn-Ets-1 constructs, have been shown to block Neu-mediated NIH 3T3 cellular transformation, and this effect is not due to dn-Ets inhibiting cellular growth (Galang *et al.*, 1994). Ets-2 may contribute to malignant transformation by inhibiting apoptosis, because Sevilla *et al.* (1999) have reported that overexpression of Ets-2 inhibits apoptosis in BAC1.2F5 macrophage cells by upregulating Bcl-x_L. Despite these advances, the ability of Ets factors to promote survival, proliferation, or transformation of mammary cells in culture has not been reported. Here we show by two separate approaches, that ESX is required for mammary cell survival. Specifically, ESX was capable of inducing colony formation in nontransformed and ESX-negative MCF-12A human mammary cells, whereas blocking ESX function via dn-ESX or antisense ESX in transformed and ESX-positive T47D cells resulted in inhibition of colony formation (Figs. 8 and 9, and Tables 1 and 2). Indeed, HA-ESX and HA-Ets-2 are both capable of inducing colony formation in MCF-12A cells with an efficiency approximating oncogenic V12Ras (Fig. 8). Of note, however, ESX overexpression in the Hs578t human breast cancer cell line was shown to have a complex effect on cellular proliferation and tumorigenesis (Choi *et al.*, 1998). In this cell line, ESX had no direct effect on cell proliferation; however, ESX apparently induced an inhibitory response to added TGF-β1 ligand and mediated a reduction in tumor size in nude mice (Choi *et al.*, 1998). This effect was most likely due to the restoration of TGFβ-II receptor expression and TGFβ1 response by ESX (Choi *et al.*, 1998). These results parallel those with PEA3, in that PEA3 has been shown to both promote and inhibit tumorigenesis in different mammary model systems, suggesting that either the level of Ets factor expressed or the recipient cell line used confers the specificity of response.

Although the colony formation assay used here does not measure cellular transformation, it does measure the ability of cells not only to plate and survive, but also to expand via proliferation into a detectable colony. Because the nontransformed MCF-12A cells are ESX-negative (data not shown) and display stringent growth factor requirements for survival and proliferation, particularly in the dilute cell conditions of the colony formation assay used here (Paine *et al.*, 1992), these cells provided a useful model to test the role of ESX in promoting cell survival and growth. Indeed, the data presented here show that the Ets factors ESX and Ets-2 promote mammary colony formation; however, these data do not address whether these Ets factors actually transform MCF-12A cells. To be presented elsewhere, we have generated MCF-12A cells stably transfected with HA-ESX and HA-Ets-2 expression vectors, and these cells display growth factor-independent proliferation and anchorage-independent cell growth (Schedin *et al.*, in preparation). Thus, taken together, our data underscore the critical importance of Ets factors, specifically ESX and Ets-2, for breast cell survival and/or growth. AU7

ACKNOWLEDGMENTS

We thank Drs. Bo Wasylyk for the 8Xpal/pBLCAT, −1100/+8 stromelysin and −517/+63 collagenase reporters,

and the pTL1-Elk-1, pSG5-Ets-1, pSG5-VP16-Ets-1, and pTL2-hNet constructs; Michael Ostrowski for the pCGN-HA-Ets-2 plasmid; and Drs. Ralph Janknecht, Frank Burton, and Tom Brown for the pSG5-ER81, pCDNA3.1-EHF, and pCMX-GABPα, and pCMX-GABPβ plasmids, respectively. We also acknowledge Drs. Dawn Duval, Andy Bradford, and Twila Jackson for critical reading of this manuscript. Tissue culture media, DNA sequencing and FACS were provided by Core Facilities of the University of Colorado Comprehensive Cancer Center (NIH P30 CA 46934). J.T.T. was supported by an NIH T32 DK074461 award and grant DOD DAMD17-97-1-7307, and S.E.D. was supported by a Postdoctoral Fellowship from the Lalor Foundation, a UCCR Seed Grant, and an NIH K01 DK02752-01 award. Boehringer Ingelheim, Austria GmbH, provided initial support for this work, and subsequent support was provided by grant DOD DAMD17-00-1-0476 to A.G.H.

REFERENCES

ALBANESE, C., JOHNSON, J., WATANABE, G., EKLUND, N., VU, D., ARNOLD, A., and PESTELL, R. (1995). Transforming p21ras mutants and c-Ets-2 activate the cyclin D1 promoter through distinguishable regions. J. Biol. Chem. **270,** 23589–23597.

ANDREOLI, J., JANG, S.-I., CHUNG, E., COTICCHIA, C., STEINERT, P., and MARKOVA, N. (1997). The expression of a novel, epithelium-specific ets transcription factor is restricted to the most differentiated layers in the epidermis. Nucleic Acids Res. **25,** 4287–4295.

ANGEL, P., IMAGAWA, M., CHIU, R., STEIN, B., IMBRA, R.J., RAHMSDORF, H.J., JONAT, C., HERRLICH, P., and KARIN, M. (1987). Phorbol ester-inducible genes contain a common *cis* element recognized by a TPA-modulated trans-acting factor. Cell **49,** 729–739.

BAERT, J., MONTE, D., MUSGROVE, E., ALBAGLI, O., SUTHERLAND, R., and DELAUNOIT, Y. (1997). Expression of the PEA3 group of Ets-related transcription factors in human breast cancer cells. Int. J. Cancer **70,** 590–597.

BENZ, C., O'HAGAN, R., RICHTER, B., SCOTT, G., CHANG, C.-H., XIONG, X., CHEW, K., LJUNG, B.-M., EDGERTON, S., THOR, A., *et al.* (1997). HER2/Neu and the Ets transcription activator PEA3 are coordinately upregulated in human breast cancer. Oncogene **15,** 1513–1525.

BRADFORD, A., and GUTIERREZ-HARTMANN, A. (1998). Ets transcription factors: Nuclear integrators of signaling pathways in the regulation of endocrine gene expression. In *Gene Engineering and Molecular Models in Endocrinology.* M. Shupnick, ed. (Humana Press, Inc., Totowa, NY), In press.

AU8

BRADFORD, A., CONRAD, K., TRAN, P., OSTROWSKI, M., and GUTIERREZ-HARTMANN, A. (1996). GHF-1/Pit-1 functions as a cell specific integrator of Ras signalling by targeting the Ras pathway to a composite Ets-1/GHF-1 response element. J. Biol. Chem. **271,** 24639–24648.

BRADFORD, A., WASYLYK, C., WASYLYK, B., and GUTIERREZ-HARTMANN, A. (1997). Interaction of Ets-1 and the POU-homeodomain GHF-1/Pit-1 reconstitutes pituitary specific gene expression. Mol. Cell Biol. **17,** 1065–1074.

BRADFORD, A.P., BRODSKY, K.S., DIAMOND, S.E., KUHN, L.C., LIU, Y., and GUTIERREZ-HARTMANN, A. (2000). The Pit-1 homeodomain and β-domain interact with Ets-1 and modulate synergistic activation of the rat prolactin promoter. J. Biol. Chem. **275,** 3100–3106.

BRADFORD, A.P., CONRAD, K.E., WASYLYK, C., WASYLYK, B., and GUTIERREZ-HARTMANN, A. (1995). Functional interaction of c-Ets-1 and GHF-1/Pit-1 mediates Ras activation of pituitary-specific gene expression: Mapping of the essential c-Ets-1 domain. Mol. Cell Biol. **15,** 2849–2857.

CHANG, C., SCOTT, G., KUO, W., XIONG, X., SUZDALTSEVA, Y., PARK, J., SAYRE, P., ERNY, K., COLLINS, C., GRAY, J., *et al.* (1997). ESX: A structurally unique Ets overexpressed early during human breast tumorigenesis. Oncogene **14,** 1617–1622.

CHANG, C.-H., SCOTT, G.K., BALDWIN, N.A., and BENZ, C.C. (1999). Exon 4-encoded acidic domain in the epithelium-restricted Ets factor, ESX, confers potent transactivating capacity and binds to TATA-binding protein (TBP). Oncogene **18,** 3682–3695.

CHOI, S.-G., YI, Y., KIM, Y.-S., KATO, M., CHANG, J., CHUNG, H.-W., HAHM, K.-B., YANG, H.-K., RHEE, H., BANG, Y.-J., *et al.* (1998). A novel Ets-related transcription factor, ERT/ESX/ESE-1, regulates expression of the transforming growth factor-β type II receptor. J. Biol. Chem. **273,** 110–117.

DELANNOY-COURDENT, A., MATTOT, V., FAFEUR, V., FAUQUETTE, W., POLLET, I., CALMELS, T., VERCAMER, C., BOILLY, B., VANDENBUNDER, B., and DESBIENS, X. (1998). The expression of Ets-1 transcription factor lacking its activation domain decreases uPA proteolytic activity and cell motility, and impairs normal tubulogenesis and cancerous scattering in mammary epithelial cells. J. Cell Sci. **111,** 1521–1534.

DITTMER, J., and NORDHEIM, A. (1998). Ets transcription factors and human disease. Biochem. Biophys. Acta **1377,** F1–F11.

DONALDSON, L., PETERSEN, J., GRAVES, B., and MCINTOSH, L. (1994). Secondary structure of the ETS domain places murine Ets-1 in the superfamily of winged helix-turn-helix DNA-binding proteins. Biochemistry **33,** 13509–13516.

DONALDSON, L., PETERSEN, J., GRAVES, B., and MCINTOSH, L. (1996). Solution structure of the ETS domain from murine Ets-1: A winged helix-turn-helix DNA-binding motif. EMBO J. **15,** 125–134.

FOOS, G., GARCIA-RAMIREZ, J., GALANG, C., and HAUSER, C. (1998). Elevated expression of Ets2 or distinct portion of Ets2 can reverse Ras-mediated cellular transformation. J. Biol. Chem. **273,** 18871–18880.

GALANG, C., DER, C., and HAUSER, C. (1994). Oncogenic Ras can induce transcriptional activation through a variety of promoter elements, including tandem c-Ets-2 binding sites. Oncogene **9,** 2913–2921.

GALANG, C., GARCIA-RAMIREZ, J., SOLSKI, P., WESTWICK, J., DER, C., NEZNANOV, N., OSHIMA, R., and HAUSER, C. (1996). Oncogenic Neu/ErbB-2 increases, Ets, AP-1 and NF-kB-dependent gene expression, and inhibiting Ets activation blocks Neu-mediated cellular transformation. J. Biol. Chem. **271,** 7992–7998.

GILLES, C., POLETTE, M., BIREMBAUT, P., BRUNNER, N., and THOMPSON, E. (1997). Expression of c-ets-1 mRNA is associated with invasive, EMT-derived phenotype in breast carcinoma cell lines. Clin. Exp. Metastasis **15,** 519–526.

GORDON, D., LEWIS, S., HAUGEN, B., JAMES, R., MCDERMOTT, M., WOOD, W., and RIDGWAY, E. (1997). Pit-1 and GATA-2 interact and functionally cooperate to activate the thyrotropin β-subunit promoter. J. Biol. Chem. **272,** 24339–24347.

GRAHAM, R., and GILMAN, M. (1991). Distinct protein targets for signals acting at the c-*fos* serum response element. Science **251,** 189–192.

GRAVES, B., and PETERSEN, J. (1998). Specificity within the *ets* family of transcription factors. In *Advances in Cancer Research.* G. Vande Woude and G. Klein, eds.

AU9

LANGER, S.J., BORTNER, D.M., ROUSSEL, M.F., SHERR, C.J., and OSTROWSKI, M.C. (1992). Mitogenic signaling by colony-stimulating factor 1 and *ras* is suppressed by the *ets*-2 DNA-binding domain and restored by *myc* overexpression. Mol. Cell Biol. **12,** 5355–5362.

LEPRINCE, D., GEGONNE, A., COLL, J., DETAISNE, D., SCHNEEBERGER, A., LARGROU, C., and STEHELIN, D. (1983). A putative second cell-derived oncogene of the avian leukemia retrovirus E26. Nature **306,** 395–397.

LIU, E., THOR, A., HE, M., BARCOS, M., LJUNG, B., and BENZ, C. (1992). The HER2 (c-erbB-2) oncogene is frequently amplified in *in situ* carcinomas of the breast. Oncogene **7,** 1027–1032.

MAXWELL, I.H., HARRISON, G.S., WOOD, W.M., and MAXWELL, F. (1989). A DNA cassette containing a trimerized SV40 polyadenylation signal which efficiently blocks spurious plasmid-initiated transcription. Biotechniques **7,** 276–280.

NEVE, R., CHANG, C.-H., SCOTT, G., WONG, A., FRIIS, R., HYNES, N., and BENZ, C. (1998). The epithelium-specific Ets transcription factor ESX is associated with mammary gland development and involution. FASEB J. **12,** 1541–1550.

NEZNANOV, N., MAN, A., YAMAMOTO, H., HAUSER, C., CARDIFF, R., and OSHIMA, R. (1999). A single targeted Ets2 allele restricts development of mammary tumors in transgenic mice. Cancer Res. **59,** 4242–4246.

ODA, N., ABE, M., and SATO, Y. (1999). ETS-1 converts endothelial cells to the angiogenic phenotype by inducing the expression of matrix metalloproteinases and integrin beta3. J. Cell Physiol. **178,** 121–132.

OETTGEN, P., ALANI, R., BARCINSKI, M., BROWN, L., AKBARALI, Y., BOLTAX, J., KUNSCH, C., MUNGER, K., and LIBERMANN, T. (1997). Isolation and characterization of a novel epithelium-specific transcription factor, ESE-1, a member of the *ets* family. Mol. Cell Biol. **17,** 4419–4433.

OETTGEN, P., BARCINSKI, M., BOLTAX, J., STOLT, P., AKBARALI, Y., and LIBERMANN, T. (1999). Genomic organization of the human ELF3 (ESE-1/ESX) gene, a member of the Ets transcription factor family, and identification of a functional promoter. Genomics **55,** 358–362.

O'HAGAN, R., and JA, H. (1998). The PEA3 Ets transcription factor is a downstream target of the HER2/Neu receptor tyrosine kinase. Oncogene **16,** 301–310.

PAINE, T.M., SOULE, H.D., PAULEY, R.J., and DAWSON, P.J. (1992). Characterization of epithelial phenotypes in mortal and immortal human breast cells. Int. J. Cancer **50,** 463–473.

PENDAS, M., BALBIN, M., LLANO, E., JIMENEZ, M., and LOPEZ-OTIN, C. (1997). Structural analysis and promoter characterization of the human collagenase-3 gene (MMP13). Genomics **40,** 222–233.

ROBINSON, L., PANAYIOTAKIS, A., PAPA, T., KOLA, I., and SETH, A. (1997). ETS target genes: Identification of egr1 as a target by RNA differential display and whole genome techniques. Proc. Natl. Acad. Sci. USA **94,** 7170–7175.

RODRIGO, I., CATO, A., and CANO, A. (1999). Regulation of E-cadherin gene expression during tumor progression: The role of a new Ets-binding site and the E-pal element. Exp. Cell Res. **248,** 358–371.

ROUSSEL, M., DAVIS, J., CLEVELAND, J., GHYSDAEL, J., and HIEBERT, S. (1994). Dual control of myc expression through a single DNA binding site targeted by ets family proteins and E2F-1. Oncogene **9,** 405–415.

SAPI, E., FLICK, M., RODOV, S., and KACINSKI, B. (1998). Ets-2 transdominant mutant abolishes anchorage-independent growth and amcrophage-stimulating factor-stimulated invasion by BT20 breast carcinoma cells. Cancer Res. **58,** 1027–1033.

SCOTT, G., DANIEL, J., XIONG, X., MAKI, R., KABAT, D., and BENZ, C. (1994). Binding of an Ets-related protein within the DNase I hypersensitive site of the HER2/neu promoter in human breast cancer cells. J. Biol. Chem. **269,** 19848–19858.

SETH, A., and PAPA, T. (1990). The c-ets-1 proto-oncogene has oncogenic activity and is positively autoregulated. Oncogene **5,** 1761–1767.

SEVILLA, L., APERLO, C., DULIC, V., CHAMBARD, J., BOUTONNET, C., PASQUIER, O., POGNONEC, P., and BOULUKOS, K. (1999). The Ets2 transcription factor inhibits apoptosis induced by colony-stimulating factor-1 deprivation of macrophages through a Bcl-x_L-dependent mechanism. Mol. Cell Biol. **19,** 2624–2634.

SHEPHERD, T., and HASSELL, J. (2000). Role of Ets transcription factors in mammary gland development and oncogenesis. J. Mammary Gland Biol. Neoplasia **6,** In press. AU10

TAKAOKA, A., YAMADA, T., GOTOH, M., KANAI, Y., IMAI, K., and HIROHASHI, S. (1998). Cloning and characterization of the human beta4-integrin gene promoter and enhancers. J. Biol. Chem. **273,** 33848–33855.

TANAKA, M., and HERR, W. (1994). Reconstitution of transcriptional activation domains by reiteration of short peptide segments reveals the modular organization of a glutamine-rich activation domain. Mol. Cell Biol. **14,** 6056–6067.

TETSU, O., and MCCORMICK, F. (1999). Beta-catenin regulates expression of cyclin D1 in colon carcinoma cells. Nature **398,** 422–426.

TREISMAN, R. (1992). The serum response element. Trends Biochem. Sci. **17,** 423–426.

TRIMBLE, M.S., XIN, J.H., GUY, C.T., MULLER, W.J., and HASSELL, J.A. (1993). PEA3 is overexpressed in mouse metastatic mammary adenocarcinomas. Oncogene **8,** 3037–3042.

TYMMS, M., NG, A., THOMAS, R., SCHUTTE, B., ZHOU, J., EYRE, H., SUTHERLAND, G., SETH, A., ROSENBERG, M., PAPAS, T., *et al.* (1997). A novel epithelial-expressed ETS gene, ELF3: Human and murine cDNA sequences, murine genomic organization, human mapping to 1q.32.2 and expression in tissues and cancer. Oncogene **15,** 2449–2462.

WASYLYK, B., and NORDHEIM, A. (1997). Ets transcription factors: Partners in the integration of signal responses. In Transcription Factors in Eukaryotes, A. Papavassiliou, ed. (Landes Bioscience), pp. 251–284. AU11

WASYLYK, C., GUTMAN, A., NICHOLSON, R., and WASYLYK, B. (1991). The c-Ets oncoprotein activates the stromelysin promoter through the same elements as several non-nuclear oncoproteins. EMBO J. **10,** 1127–1134.

WASYLYK, B., HAGMAN, J., and GUTIERREZ-HARTMANN, A. (1998). Ets transcription factors: Nuclear effectors of the Ras/MAP kinase signaling pathway. Trends Biochem. Sci. **23,** 213–216.

WASYLYK, C., MAIRA, S.-M., SOBIESZCZUK, P., and WASYLYK, B. (1994). Reversion of Ras transformed cells by Ets transdominant mutants. Oncogene **9,** 3665–3673.

WATABE, T., YOSHIDA, K., SHINDOH, M., KAYA, M., FUJIKAWA, K., SATO, H., SEIKI, M., ISHII, S., and FUJINAGA, K. (1998). The Ets-1 and Ets-2 transcription factors activate the promoters for invasion-associated urokinase and collagenase genes in response to epidermal growth factor. Int. J. Cancer **77,** 128–137.

XING, X., WANG, S.C., XIA, W., ZOU, Y., SHAO, R., KWONG, K.Y., YU, Z., ZHANG, S., MILLER, S., HUANG, L. *et al.* (2000). The Ets protein PEA3 suppresses Her-2/neu overexpression and inhibits tumorigenesis. Nat. Med. **6,** 189–195.

ZHANG, M., MAASS, N., MAGIT, D., and SAGER, R. (1997). Transactivation through Ets and AP1 transcription sites determines the expression of the tumor-supressing gene maspin. Cell Growth Diff. **8,** 179–186.

Address reprint requests to:
Arthur Gutierrez-Hartmann AU12
University of Colorado Health Sciences Center
4200 East Ninth Avenue, Box B-151
Denver, CO 80262

E-mail: a.gutierrez-hartmann@uchsc.edu

Received for publication July 2, 2002; received in revised form October 30, 2002; accepted October 30, 2002. AU13

ESX Induces Transformation and Functional Epithelial to Mesenchymal Transition in MCF-12A Mammary Epithelial Cells

Pepper J. Schedin, Kristin L. Eckel, Shauntae M. McDaniel, Jason D. Prescott,

Kelley S. Brodsky, John J. Tentler and Arthur Gutierrez-Hartmann*

Departments of Medicine and of Biochemistry & Molecular Genetics, Program in Molecular Biology, and Colorado Cancer Center, University of Colorado Health Sciences Center

*To whom correspondence should be addressed:

Arthur Gutierrez-Hartmann, MD
University of Colorado Health Sciences Center
4200 East Ninth Avenue, Box B-151
Denver, CO 80262

Oncogene, accepted

Telephone: 303-315-8443
FAX: 303-315-4525
Email: a.gutierrez-hartmann@uchsc.edu

Running Title: ESX transforms mammary epithelial cells

Abstract

ESX is an epithelial-restricted member of a large family of transcription factors known as the Ets family. ESX expression has been shown to be correlated with Her2/neu proto-oncogene amplification in highly-aggressive breast cancers and induced by Her2/neu in breast cell lines, but it's role in tumorigenesis is unknown. Previously we have shown that ESX enhances breast cell survival in colony formation assays. In order to determine whether ESX can act as a transforming gene, we stably transfected MCF-12A human epithelial mammary cells with the ESX expression vector, pCGN2-HA-ESX. The MCF-12A cell line is immortalized, but nontransformed, and importantly, these cells fail to express endogenous ESX protein. We used pCGN2-HA-Ets-2 and pSVRas expression vectors as positive controls for transformation. Stable expression of ESX induced EGF-independent proliferation, serum-independent MAPK phosphorylation and growth in soft agar. Additionally, stable ESX expression conferred increased cell adhesion, motility and invasion in two-dimensional and trans-well filter assays, and an epithelial to mesenchymal morphological transition. In three-dimensional cultures, parental and vector control (pCGN2) cells formed highly organized duct-like structures with evidence of cell polarity, ECM adhesion-dependent proliferation and cell survival, and lack of cellular invasion into surrounding matrix. Remarkably, the ESX stable cells formed solid, disorganized structures, with lack of cell polarity and loss of dependence on ECM adhesion for cell proliferation and survival. In addition, ESX cells invaded the surrounding matrix, indicative of a transformed and metastatic phenotype. Taken together, these data show that ESX expression alone confers a transformed and in vitro metastatic phenotype to otherwise normal MCF-12 cells.

Introduction

The ETS family is a large group of transcription factors that are known to play significant roles in development, differentiation, and transformation (Graves & Petersen, 1998; Wasylyk et al., 1998). ETS family members are defined by the ETS domain, a highly-conserved, 85 amino acid DNA-binding domain (DBD) that is folded into a novel winged helix-turn-helix DNA-binding motif (Donaldson et al., 1994; Donaldson et al., 1996). ESX, also known as ESE-1, Ert, Jen and Elf-3, is unique among ETS members with regards to its expression and its structure. Specifically, its expression is restricted to epithelial cells and the protein contains two additional motifs, a serine-rich box and an AT-hook domain (Benz et al., 1997; Chang et al., 1997; Chang et al., 1999; Oettgen et al., 1997). The founding member of the ETS family, the v-*ets* oncogene from the E26 retrovirus, causes hematopoetic malignancies in chickens (Leprince et al., 1983). An important aspect of this family of transcription factors is that several ETS members have also been identified as critical components of the cellular pathways leading to tumorigenesis in humans (Dittmer & Nordheim, 1998; Wasylyk et al., 1998).

Several different lines of evidence suggest that ETS factors play a particularly relevant role in breast cancer. For example, ETS factor over-expression has been reported in human and rodent mammary tumor biopsies and cell lines, including members of the ETS-1, PEA-3 and ESX genes (Baert et al., 1997; Benz et al., 1997; Dittmer & Nordheim, 1998; Gilles et al., 1997; Shepherd & Hassell, 2000; Watabe et al., 1998). Moreover, expression of dominant-negative (dn) Ets DBD constructs has been shown to completely block the anchorage-independent growth and cellular invasiveness of MMT and BT20 breast carcinoma cell lines (Delannoy-Courdent et al., 1998; Sapi et al., 1998). These results provide compelling data supporting a direct role of ETS proteins in transformation of mammary epithelial cells. Of these various ETS factors, ESX

has been recently implicated as a key transcription factor associated with human breast cancer (Chang et al., 1997; Liu et al., 1992; Tymms et al., 1997). For example, ESX has been shown to be amplified in ~50% of early breast tumors (Tymms et al., 1997) and ESX expression is significantly increased in ductal carcinoma in situ (DCIS) (Chang et al., 1997; Liu et al., 1992). Furthermore, there is a positive correlation between ESX and HER2/neu proto-oncogene expression in human breast cancers, and this co-expression strongly correlates with a highly metastatic phenotype and poor prognosis (Benz et al., 1997; Chang et al., 1997; Liu et al., 1992). A positive-feedback-regulatory loop between HER2/neu and ESX has been suggested by the demonstration that HER2/neu activation induced ESX expression while the Her2/neu promoter can be activated by ESX via an ETS-like DNA sequence motif (Benz et al., 1997; Eckel et al., 2003; O'Hagan & JA, 1998). While these studies clearly implicate ETS factors in breast cancer, the ability of any specific ETS factor, including ESX, to actually transform normal breast cells has not been shown.

To investigate the potential roles of ESX in breast cell transformation and acquisition of metastatic potential, we generated stable transfectants of MCF-12A human mammary epithelial cells expressing ESX, Ets-2 and V12-Ras. We chose MCF-12A cells as the model system, since these cells are immortalized, but nontransformed human mammary epithelial cells (Paine et al., 1992) that fail to express ESX (see below). In this paper, we focused on functional assays that measure cellular transformation and metastatic potential, with particular emphasis on examining the epithelial-to-mesenchymal transition (EMT). The rationale for this emphasis is that EMT has been strongly correlated with multiple events in the metastatic cascade, including the ability of tumor cells to disseminate from the primary tumor, to intravasate into vasculature or lymphatics, and to extravasate into tissue at secondary sites(Hay, 1995; Horwitz et al., 1995; Kantor & Zetter, 1996). At the cellular level, EMT involves loss of epithelial characteristics, such as apical-basal cell polarity

and cell-cell adhesion junctions, and gain of mesenchymal characteristics, such as motility and invasiveness; all attributes that are readily measurable in vitro (Kantor & Zetter, 1996). Here we show that stable expression of ESX is sufficient to confer a transformed and in vitro metastatic phenotype to otherwise normal, but immortalized MCF-12 cells, suggesting that ESX may be a critical downstream effector of the HER2/neu pathway.

Materials and Methods

Plasmid Constructs- A cDNA spanning the coding sequence of human ESX mRNA was amplified by RT-PCR and subcloned into pCR2.1 (Invitrogen Corporation), as previously described (Eckel et al., 2003). The ESX cDNA sequence and its orientation were verified by dideoxy sequencing at the UCHSC Cancer Center DNA Sequencing Core facility. ESX was excised from pCR2.1-ESX by digestion with Bgl II and Afl III, and the 1116 base pair Bgl II ESX fragment was ligated into a BamH I linearized and dephosphorylated pCGN2-HA vector (Bradford et al., 2000) to generate pCGN2-HA-ESX (Eckel et al., 2003). The plasmid pCGN-HA-Ets-2 was provided by Dr. Michael Ostrowski (Ohio State University).

Cell line culture conditions- MCF-12A cells were obtained from ATCC (Manassas, VA). For routine maintenance, cells were grown in complete media consisting of Ham's F12/Dulbecco modified Eagle media (DMEM; Gibco/BRL) containing 100 ng/ml cholera toxin (Gibco/BRL), 0.5 μg/ml hydrocortisone (Sigma), 10 μg/ml insulin (Sigma), 20 ng/ml EGF (Sigma), and 5% horse serum (Gibco/BRL).

RT-PCR- MCF-7, MCF-12A wild-type, pCGN2-P, ESX-P, Ets-2-P and V12Ras-P cells were grown to 80-90% confluency and harvested with 1 X PBS and 3 mM EDTA. Total RNA was isolated using an RNA STAT-60 kit (Teltest, Friendswood, TX). Expression of endogenous ESX was determined using oligos specific for the 5' and 3' ends of the ESX coding region (Eckel et al., 2003). Similarly, expression of HA-ESX mRNA was determined using oligos directed to the HA tag and the carboxy-terminus of ESX (Eckel et al., 2003), thus allowing the selective amplification of the exogenous, recombinant HA-ESX mRNA.

Stable Cell Lines- Immortalized but non-transformed MCF-12A human mammary epithelial cells were transfected by electroporation with 2 μg of pRSVneo and either 20 μg of control pCGN2 vector, pCGN2-HA-ESX, pCGN2-HA-Ets-2 or pSV-Ras (oncogenic V12-Ras). Following electroporation, cells were immediately plated into 60 mm dishes with 3 ml of complete media, as described above. After a 24 hour incubation in 95% O_2 and 5% CO_2 at 37^0 C, media was replaced with fresh Ham's F12/DMEM containing all of the supplements listed above, as well as 500 μg/ml G418 in order to select for geneticin-resistant cells. After two weeks of selection, pools of G418-resistant cells, denoted as pCGN2-P, ESX-P, Ets-2-P, and V12Ras-P, were re-plated, expanded and maintained in complete media containing 200 μg/ml G418. For experiments described, log phase cells between passages 4-10 were utilized.

Phospho-MAP Kinase Assays- Stable cell lines were starved for sixteen hours in media containing 0.1% serum and no EGF. Cells were then harvested by lysis directly on the plate with 2 X SDS protein load dye (Owl Separation Systems) consisting of 0.25 M Tris/HCl pH 6.8, 2% SDS, 10% β-mercaptoethanol, 30% glycerol, and 0.01% bromophenol blue. Lysates were sheared with a 25G needle and boiled for five minutes before loading onto a 10% SDS polyacrylamide gel and analysed with a phospho-p44/42 MAP kinase antibody (New England Biolabs) by Western blot, performed as described above.

Cell Growth Assay- Cells were harvested from sub-confluent plates and were resuspended in complete media and plated in 24 well plates at a density of 10,000 cells per well. After 24 hours, cells were harvested from the first plate and counted on a hemocytometer. Media was changed on the remaining cells to F12/DMEM with reduced serum (1%) and no EGF, or media with reduced serum (1%) and the addition of 20 ng/ml EGF. This restricted media was replaced on cells every 24 hours in order to prevent growth factor accumulation from neighboring cells. Cells

were harvested every 24 hours for 5 days and cell number determined by counting on a hemocytometer.

Soft Agar Assay- Stable pools were harvested at 80-90% confluency and counted. A base layer of 0.35% low melting point agarose (SeaPlaque) in 1X DME (Gibco/BRL) and 10 % horse serum (Gibco/BRL) was poured into 60 mm plates and allowed to harden at 4°C. Twenty thousand cells of each stable cell line were resuspended in complete media plus agar mixture at 42°C and seeded on top of the solidified base layer. Plates were incubated at 37°C in 95% O_2 and 5% CO_2 for 4 weeks. Plates were fed drop-wise with complete media as needed, to keep the agar mixture from drying out. After four weeks, plates were photographed at 40X for maximal colony visibility.

Adhesion Assay – Log phase cells were harvested with trypsin-EDTA and re-suspended at 60,000 cells per well in 96 well tissue culture plates (Nunclon) in complete medium supplemented with G418 (200 μg/ml). After 30, 45, 60, and 75 minutes of incubation at 37° C, cells were rinsed 3X with Hank's Buffered Salt Solution (HBSS) to remove non-adhered cells. Adhered cells were fixed with 10% neutral buffered formalin (NBF) for 5 minutes, stained with 0.1% crystal violet for 5 minutes, rinsed twice with HBSS to remove any unabsorbed stain, and air-dried. The number of adhered cells was determined using an optical density method previously described (Bernhardt et al., 1992), with slight modifications. Briefly, crystal violet was extracted from stained cells by adding 180 μl of 70% ethanol per well, followed by rocking at RT for 2 hr. Optical density of the extracted crystal violet was read at 590 nm. Each cell line and each time point were performed in quadruplicate. Data are expressed as mean ± s.e.m. For determination of percent cells adhered, a standard linear curve was generated by measuring the optical density of extracted crystal violet from known cell concentrations.

Scrape Assay – Log phase cells were placed in 60 mm tissue culture plates and grown to 100% confluency in complete medium supplemented with G418. The plates were rinsed in HBSS and a line of cells was removed from the center of the plates using a 1000 μl pipet tip. Free floating cells, dislodged from the scrape line, were removed by rinsing with HBSS. Culture media free of serum and EGF was added and plates incubated for 24 hours at 37°C. To visualize motile cells within the scrape line, cells were fixed with 10% NBF for 5 minutes, stained with 0.1% crystal violet for 5 minutes, and excess stain removed with water. Cells were viewed on a Zeiss Axioscope 25 microscope and representative scrape lines for each cell line photographed. All conditions were performed in triplicate and experiment performed in duplicate.

Transwell Filter Motility Assay- Transwell tissue culture filters with 8.0 μm pore size (Falcon #3097) were pre-coated with 50 μl of 10 μg/ml porcine gelatin (Sigma), which was allowed to solidify overnight at room temperature. Log phase cells were harvested with trypsin-EDTA and re-suspended in complete medium supplemented with only 0.1% horse serum. Fifty-thousand (50,000) cells per well were overlaid onto the top of the transwell filters (24 well format). Cells were stimulated to migrate across the filters by providing a chemoattractant (0.6% horse serum) in the assay chambers beneath the coated filter. After a 4 hour incubation at 37°C, cells were fixed in 10% NBF for 5 minutes and stained with 0.1% crystal violet for 5 minutes. Non-motile cells on the top of the filter were removed by gentle scraping and cells that crossed through the filter pores were quantified photographically as previously reported (Bemis & Schedin, 2000). All conditions were performed in triplicate and experiment performed in duplicate. Data are expressed as mean ± s.e.m.

Invasion Assay- Transwell filters were coated with 50 μl of 200 μg/ml porcine gelatin (Sigma) and allowed to solidify overnight to occlude the 8.0 μm pores. Cells were suspended at 50,000

cells per well in 24-well filter plates (Falcon) using two different culture media, designed to evaluate growth factor dependency of invasion. The least restrictive media contained Ham's F12/DMEM (Gibco/BRL) supplemented with 0.1% horse serum, 10 μg/ml insulin, 500 ng/ml hydrocortisone, 20 ng/ml EGF, 100 ng/ml cholera toxin, and 200 μg/ml G418. The highly restrictive media consisted of Ham's F12/DMEM without any supplementation. Horse serum (0.6%) was utilized as the chemoattractant in the lower chamber. The number of invasive cells, evaluated 24 hours after plating, was quantified as for motility assay. All conditions were performed in triplicate and experiment performed in duplicate. Data are expressed as mean ± s.e.m.

3-Dimensional (3-D) Culture Model- Log phase cells in complete medium plus G418 were overlaid as a single cell suspension onto a 100 μl matrix substratum using 30,000 cells per well (96-well tissue culture plate; Nunclon). The matrix substratum consisted of a 1:1 mixture of Matrigel (Collaborative Biomedics) and complete medium plus G418. The development of organoids in this 3-D model is dependent on the migration of single cells into cell aggregates as previously described (Bemis & Schedin, 2000). Organoid development was monitored over 96 hours by inverted-light microscopy (Zeiss Axioscope 25) and photographed with a Polaroid camera at 100 X. After 72 hours, the organoids were treated with 0.01 mM of bromodeoxyuridine (BrdU) (Sigma) for 24 hours. Organoids were harvested at 96 h post-plating, stained with 0.1% trypan blue, fixed in methacarn for 10 minutes, paraffin embedded, and cut into 5 μm sections.

Immunohistochemical detection of BrdU- Slides with 5 μm sections were heat fixed for 20 minutes at 80°C. After clearing in xylene, tissue sections were rehydrated and endogenous peroxidase activity blocked with 3% peroxide. Slides were incubated in a 1:40 dilution of anti-

BrdU (Beckton Dickinson) in PBS for 1 hour followed by incubation in a 1: 200 dilution of biotinylated rabbit anti-mouse secondary antibody (Dako) in PBS for 30 minutes. Biotin was detected by incubation in a 1:1000 dilution of conjugated HRP-streptavidin (Gibco/BRL), followed by 10 minutes in 0.6 mg/ml of DAB (3,3'-diaminobenzidine tetrahydrochloride) in 20 μl of 3% peroxide. Slides were counter-stained using a 1:10 dilution of Harris hematoxylin, rinsed with Scott's water, dehydrated in a series of ethanols, cleared in xylene, and then mounted with permount. The percentage of cells that incorporated BrdU was determined as previously described (Schedin et al., 2000). Briefly, 20 randomly chosen fields were selected per cell line and photographed. The percent BrdU-positive cells that stained dark-brown, were counted from coded photographs independently by two investigators. Data are expressed as mean ± s.e.m.

Results

Characterization of the Stable Pooled Cell Lines

In order to test the hypothesis that ESX imparts a transformed phenotype upon human mammary epithelial cells, we required a human mammary epithelial cell line that displays essentially a nontransformed phenotype and that does not express ESX. The MCF-12A cell line fulfills these criteria. MCF-12A cells are a mixed population of epithelial cells that grow as patches of organized cuboidal cells surrounded by fibroblast-like cells in culture (Paine et al., 1992). They are EGF-dependent for proliferation, fail to grow in an anchorage-independent manner and fail to produce tumors in nude mice (Wang et al., 1997). To verify that MCF-12A cells failed to express ESX, we performed RT-PCR analysis using oligonucleotide primers specific for the endogenous ESX mRNA in MCF-7 cells, as positive control, and in MCF-12A cells (Fig. 1A). The results show that endogenous ESX is detected in MCF-7 cells with as few as

20 cycles, whereas no ESX RT-PCR product was detected in MCF-12A cells with as many as 35 cycles (Fig. 1A).

Having verified that MCF-12A cells do not express ESX, these cells were stably transfected with pCGN2-HA-ESX, to evaluate the effects of ESX expression on mammary cell transformation. As a positive control for transformation, we used pSV-Ras, which encodes the V12Ras oncogene and has been shown to confer the transformed phenotype in MCF-12A cells (Wang et al., 1997). In addition, over-expression of the ETS family member, Ets-2, has been correlated with mammary tumorigenesis, but its precise role remains in question (Neznanov et al., 1999). Thus, we used pCGN2-HA-Ets-2, which encodes an HA-tagged version of Ets-2, to compare its effects with those of ESX and V12Ras. The pCGN2 control vector, pCGN2-HA-ESX, pCGN2-HA-Ets-2 or pSV-Ras plasmid DNAs were individually transfected into MCF-12A cells. Stable transfectants were selected and approximately 200 stably transfected clones were pooled to establish pooled cell lines denoted as pCGN2-P, ESX-P, Ets-2-P and V12 Ras-P. We chose to focus our study on pooled, stable transfectants, rather than clonal isolates, since the parental MCF-12A population is morphologically heterogenous and this heterogeneity appears to contribute to the normal, nontransformed phenotype (Kordon & Smith, 1998; Paine et al., 1992).

To verify the expression of exogenous HA-ESX in the stable ESX-P cells, we performed RT-PCR analysis using oligonucleotide primers specific for the HA-tagged ESX cDNA. Figure 1B, lanes 1 and 2 show two negative controls, demonstrating that neither the solutions of the PCR or reverse trancriptase (RT) reactions contained HA-ESX mRNA or DNA contaminants, respectively. Lanes 3 and 4 (Fig. 1B) show that neither nontransfected parental MCF-12A cells or vector control pCGN2-P cells, respectively, express detectable levels of HA-ESX mRNA. By contrast, HA-ESX mRNA was readily detected in ESX-P cells (Fig. 1B, lane 5). DNA

sequencing of the upper, dominant band verified that the product was indeed authentic HA-ESX (data not shown). Also, Fig. 1B, lanes 6 and 7, reveal that Ets-2-P and V12Ras-P cell lines failed to express HA-ESX mRNA. In addition, we verified that exogenous HA-Ets-2 was expressed in the Ets-2-P cells using a similar RT-PCR strategy (data not shown). Finally, lane 8 shows the PCR product of a positive control, using pCGN-ESX plasmid DNA as the PCR template.

ESX, Ets-2 and V12Ras Confer EGF-Independent Growth

The parental MCF-12A cells have been reported to be highly dependent on exogenous EGF for cell growth (Paine et al., 1992). One characteristic of cellular transformation is loss of growth factor dependence (Hanahan & Weinberg, 2000). In order to evaluate the EGF dependence of pCGN2-P, ESX-P, Ets-2-P and V12Ras-P cells for growth, we determined the growth rates of each of these cell populations in media containing reduced serum (1% horse serum) in the presence or absence of EGF (20 ng/ml). As shown in Figure 2A, the parental nontransfected MCF-12A and the pCGN2-P cells had a limited ability to grow in media that lacked EGF, whereas cell number of ESX-P, Ets-2-P and V12-Ras-P cells increased 4-fold relative to parental or pCGN2-P controls by day 6. Indeed, by the fifth day, the number of cells in control cultures was declining, while the cell number in ESX-P, Ets-2-P and V12-Ras-P cultures continued to increase. The differences in cell number between control and experimental lines is unlikely to be attributed to differential plating efficiency, since the number of adhered cells 24 hours after initial plating of these various cell lines was statistically indistinguishable from each other (Fig. 2A, 1 day). However, in EGF-containing media, the ESX-P, Ets-2-P and V12-Ras-P cells respond to exogenous EGF as demonstrated by a 5-fold increase in cell number in EGF-containing media (Fig. 2A) compared to EGF-depleted media (Fig. 2B). Therefore,

transfection of ESX, Ets-2 or V12-Ras did not confer a significant growth advantage when cells were plated in EGF-containing media. Cumulatively, these data indicate that stable expression of ESX, Ets-2 and V12-Ras imparts a survival advantage to MCF-12A cells under EGF-depleted conditions, rather than conferring a dominant proliferative advantage, since there is a difference in the absolute cell number achieved ± EGF.

Phosphorylated Levels of MAP Kinase in Stable Populations

Having shown that ESX-P, Ets-2-P and V12-Ras-P cells had a growth advantage in EGF-depleted media (Fig. 2A), we hypothesized that an autocrine loop had been established in MCF-12A cells by the expression of ESX, Ets-2 and V12-Ras. If this was the case, then downstream signaling molecules, such as MAP kinase, should be in the active, phosphorylated state even in the absence of EGF and serum. To determine the levels of phosphorylated MAP kinase in pCGN2-P, ESX-P, Ets-2-P and V12-Ras-P cells, these lines were grown in serum-depleted (0.1%) media lacking EGF. Under these growth conditions, the untransfected MCF-12A and vector control pCGN2-P cells displayed little to no detectable levels of phosphorylated MAP kinase (Fig. 3, top panel). In contrast, in these serum-starved and growth factor-depleted conditions, the ESX-P, Ets-2-P and V12-Ras-P cells displayed readily detectable levels of phosphorylated MAP kinase. The data in Fig. 3 was quantitated by densitometry and normalized to the actin levels, and revealed that phospho-MAPK levels were equivalent for the ESX-P and Ets-2-P cells and that these levels were approximately 20-fold greater than that of vector control cells (data not shown). Of note, the V12-Ras-P cells displayed a 200-fold increase in phospho-MAPK levels compared to controls cells (data not shown). These data are consistent with the cell number data (Fig. 2A), and suggest that ESX, Ets-2 and V12-Ras have each established an

autocrine loop, resulting in constitutive phosphorylation of MAPK to cells under growth-restrictive conditions.

Anchorage-independent Growth of ESX-P, Ets-2-P and V12-Ras-P Cells in Soft Agar

The transfection of constitutively active Ras into WT MCF-12A cells with has been shown to give these cells the ability to form colonies in soft agar (Wang et al., 1997). Such anchorage-independent growth is an accepted indicator of transformation (Hanahan & Weinberg, 2000). In order to assess the transformation potential of HA-ESX and HA-Ets-2 in MCF-12A cells, the ability of stable pooled populations of cells to form colonies in the restrictive soft agar assay was determined. At four weeks, vector control plates had very few detectable colonies (Fig. 4, pCGN2-P). HA-ESX transfectants had numerous small (0.1 mm) to medium (0.6 mm) foci (Fig. 4, ESX-P). HA-Ets-2 and V12-Ras stable cells had fewer, but larger foci ranging from 0.5 to 2 mm, which were easily detectable with the naked eye (Fig. 4, Ets-2-P andV12Ras-P).

ESX, Ets-2 and V12Ras Confer a Functional Mesenchymal Phenotype in MCF-12A Cells

A hallmark characteristic of highly metastatic epithelial tumor cells is the acquisition of a mesenchymal phenotype (Hay, 1995). In order to determine whether ESX, Ets-2 or V12-Ras are able to induce a functional epithelial to mesenchymal transition in MCF-12A cells, we measured cellular properties associated with the mesenchymal phenotype, including adhesion, motility and invasiveness. Figure 5 shows that 75 min after initial plating, ~25% of pCGN-2-P control cells were adhered, while ~70% of the ESX-P and Ets-2-P cells were adhered. The V12-Ras-P cells adhered more rapidly (50% at the earliest time point of 30 min) and more completely (essentially

100% by 45 min). At 24 hours after plating, the plating efficiency was equivalent for all cell lines (data not shown), an observation consistent with data presented in Fig. 2.

Having established increased adhesiveness of the ESX-P, Ets-2-P and V12-Ras-P cells, we next evaluated whether these cells also displayed increased motility. In the scrape motility assay, confluent cultures were wounded by scraping cells to expose a linear cell-free zone. The cell motility that is measured in the scrape assay relies on the ability of cells to overcome cell-cell and cell-substratum interactions. In the culture conditions used here, we minimized the contribution of cell proliferation to the re-population of the scrape zone, by utilizing serum-free and growth factor-depleted media. The ability of cells to re-populate this zone was measured 24 hours after wounding (Fig. 6A). In serum-free culture conditions, pCGN2-P cells failed to re-populate this zone (Fig. 6A, upper left), while ESX-P and Ets-2-P cells re-populated approximately 50% of the scraped zone (Fig. 6A, upper right and lower left). The V12-Ras-P cells displayed the highest motility and were able to re-populate the entire zone within 24 hr (Fig. 6A, lower right).

Visual inspection of the scrape zone revealed notable differences in cell morphology between the cell lines. The pCGN2-P cells produced two distinct morphological phenotypes, a densely packed, darkly stained cuboidal-like epithelial cell that formed distinct islands (Fig. 6A, upper left, wide arrows) and more loosely packed, lightly stained elongated cells that surrounded these islands (fine arrow). These two distinct cell phenotypes have been previously described for MCF-12A cells (Paine et al., 1992). Remarkably, in the ESX-P, Ets-2-P and V12-Ras-P cells there is a selective loss of the cuboidal islands, while the fibroblast-like cells were maintained (Fig. 6A). Of note, the V12-Ras-P cells acquired additional morphological features, manifested by a higher degree of homogeneity and a particularly elongated cell shape.

To gain further insights of the motile properties gained by ESX expression, we also tested MCF-12A cell motility using the short-term (4 hr) trans-well assay, wherein the ability of single cells to migrate independent of cell interactions and in response to a chemo-attractant is measured. As shown in Fig. 6B, the pCGN2-P vector control cells displayed very low motility (~12 cells/field; set to 1), while the ESX-P cells revealed approximately 6.5-fold increased motility (~80 cells/field). The Ets-2-P cells (~48 cell/field) also demonstrated a 4-fold increased motility compared to control pCGN2-P cells, but an apparent reduced motility compared to ESX-P cells. The V12-Ras-P cells showed the highest motility (~150 cells/field; 11.5-fold). Thus, using two different experimental approaches to measure cell motility, we detected an increased motility in the ESX-P, Ets-2-P and V12-Ras-P cells in comparison to control pCGN2-P cells. Analysis of cell morphology in the trans-well assay revealed that the ESX-P and ETS-2-P cells had very different cell shape compared to the V12-Ras-P cells. Figure 7 shows representative fields of the bottom of trans-well filters, stained with crystal violet. The upper left panel shows that very few pCGN2-P cells migrated through the filter. The arrow points to a filter pore, and a single stained motile cell is noted just above and to the left of the arrow. The ESX-P panel shows numerous migratory cells, and these cells acquired a flattened morphology with increased surface area and prominent broad lamellapodia (arrow). Panel Ets-2-P depicts cells with both large ruffled lamellopodia (arrow) and occasional thin filopodia. In contrast, the morphology of the V12Ras-P cells was highly elongated and fibroblast-like, with two to three prominent filopodia per cell (arrow).

Having established that the ESX, Ets-2 and V12-Ras genes conferred a motile phenotype to MCF-12A cells, we next sought to determine whether these various stable cell lines displayed enhanced invasive properties. The method used to test for invasion was the trans-well filter 24

hour invasion assay. In this assay, cells are over-layed onto filters in which the 8 μm pores are occluded with gelatin so that the transit of cells to the lower chamber requires both active matrix degradation and motility. Figure 8 shows that, independent of media conditions, control pCGN2-P cells displayed low invasion (~40-50 cells/field), while the ESX-P, Ets-2-P and V12Ras-P displayed marked invasion that ranged from 3-6-fold over controls (Fig. 8). These results demonstrating invasiveness in the absence of growth factors are in agreement with our previous data showing that the ESX-P, Ets-2-P and V12Ras-P cells are able to proliferate and activate MAPK in growth factor-depleted conditions and are consistent with the idea that an autocrine loop has been established by the expression of ESX, Ets-2 or V12Ras.

MCF-12A Cells Recapitulate Normal Mammary Development in a 3D Culture Assay

We sought to expand the utility of the MCF-12A cell system by establishing an in vitro, three-dimensional (3D) culture assay designed to mimic normal mammary development in vitro. Our rationale for this approach was that 3D assays have been demonstrated to rapidly distinguish between transformed and nontransformed mammary epithelial cells in culture (Weaver et al., 1996). For our studies, we sought to determine the effects of ETS transcription factors and oncogenic V12Ras on the ability of MCF-12A cells to develop into mammary duct-like structures. In order to address this question, we first needed to establish whether MCF-12A cells were capable of recapitulating normal mammary gland-like structures in 3D culture. Single cell suspensions of MCF-12A cells were overlayed onto reconstituted basement membrane substratum (Matrigel) and organoid development analyzed, as previously described (Bemis & Schedin, 2000). Within the first 24 hours, MCF-12A cells were observed to aggregate into solid 3-dimensional mammary-like structures (data not shown). Between 24 and 72 hours, these

organoids hollowed into both alveolar- and duct-like structures with central lumens, as shown in Fig. 9A, left panels. An alveolar-like structure is depicted in the upper left panel with the asterisks denoting cavitation and the arrow pointing to an apoptotic cell. In comparison to parental MCF12A cells, the pCGN2-P cells organized only into duct-like structures (Fig. 9A, right panels). In addition, fewer of these pCGN2-P organoids hollowed (Fig. 9A, upper right panel). However, both the parental MCF-12A and pCGN2-P cells maintained several features of normal mammary-like epithelium, including morphological evidence of lumen formation, apical-basal polarity, cell-cell adhesions, organoid size (ie, organoids that approximate in vivo duct and alveolar size) and lack of invasiveness into surrounding matrix.

ESX-P, Ets-2-P and V12Ras-P Cells Form Aggressive Tumor-Like Structures in 3D Culture

Having established that MCF-12A and control pCGN2-P cells were capable of forming normal mammary gland-like structures in a 3D cultures, we next determined the ability of ESX-P, Ets-2-P and V12Ras-P cell lines to organize in 3D culture. All three of these cell lines formed disorganized solid structures consistent with an aggressive, tumor-like phenotype (Fig. 9B). Within the first 24 hours, the ESX-P, Ets-2-P and V12Ras-P cell lines formed large, solid organoids that lacked cell polarity and failed to hollow, because unlike parental MCF-12A cells, internal cells failed to die (Fig. 9B, top and left three panels). Failure of internal cells to undergo apoptosis is further evidence that ESX-P, Ets-2-P and V12Ras-P cells are anchorage-independent for cell viability. Moreover, many of the tumor-like organoids formed by these cell lines were much larger than those formed by the parental and pCGN-2P cells (compare top panel of Fig. 9B to Fig. 9A). This result indicates that these tumor-like organoids failed to appropriately limit the number of cells contributing to each organoid, an attribute previously identified in tumorigenic

mammary epithelial cells in 3D culture (Weaver et al., 1996). By 72 hours, the ESX-P, Ets-2-P and V12Ras-P organoids exhibited features not seen in control organoids. Specifically, cells from the ESX-P, Ets-2-P and V12Ras-P organoids had locally invaded their surrounding matrix (Fig. 9B, right three panels, arrowheads). In addition to acquisition of motility and invasiveness, these invasive cells displayed further evidence of EMT, as shown by their loss of adhesion to neighboring cells and acquisition of fibroblast-like shape with prominent invasive filopodia (Fig. 9B, arrowheads).

ESX-P, Ets-2-P and V12Ras-P Cells Have Reduced Proliferation Rates in 3D Culture

As shown in Fig. 2, we have demonstrated that the ESX-P, Ets-2-P and V12Ras-P cells have a survival advantage in EGF-depleted media. Because the 3D culture conditions more closely mimic the in vivo cell-cell and cell-substratum architecture, we sought to determine the effects of ESX, Ets-2 and V12Ras gene expression on the proliferation rates of these cells in the 3D-culture model. Contrary to our expectations, morphological analysis of 5 μm sections of organoids revealed decreases BrDU incorporation in ESX-P, Ets-2-P and V12Ras-P cells , compared to control pCGN-2-P cells (Fig. 10A). In the pCGN-2-P cells, BrDU incorporation was preferentially localized to those cells at the periphery of the organoid (Fig. 10A, upper left panel, arrow), indicating that proliferation occurred in cells contacting the matrix substratum. By contrast, BrDU incorporation in the ESX-P (upper right panel), Ets-2-P (lower left panel) and V12Ras-P (lower right panel) cells was scattered and random throughout the solid tumor-like lesion (large arrows). Of interest, ESX-P, Ets-2-P and V12Ras-P cells that displayed the EMT phenotype and that had migrated away from the central solid tumor, were not observed to incorporate BrDU (Fig. 10A, arrowheads). Quantitation of BrDU incorporation revealed that

ESX-P, Ets-2-P and V12Ras-P cells displayed proliferation rates that were ~5- to 6-fold lower compared to that of the pCGN-2-P control cells (Fig. 10B). Specifically, in a 24 hour period, 32% of the pCGN-2-P cells displayed proliferation (Fig. 10B). Whereas the percent of ESX-P, Ets-2-P and V12Ras-P cells that incorporated BrDU was much lower, measuring 5%, 8% and 13%, respectively (Fig. 10B).

Discussion

This paper provides several key contributions that further our understanding of transformation of mammary epithelial cells by Ets factors. Importantly, this is the first demonstration of the ability of transfected Ets DNA to act as a transforming gene in mammary epithelial cells in vitro. Here, we show that the Ets factors ESX and Ets-2 are each capable of conferring aggressive, metastatic properties to immortalized, but nontumorigenic human mammary epithelial MCF-12A cells. Specifically, ESX and Ets-2 stably-transfected MCF-12A cells acquired growth factor- and anchorage-independent growth, and displayed enhanced motility and invasiveness in 2D and 3D culture. Moreover, in 3D organoid assays, it was evident that ESX and Ets-2 induced a functional epithelial-to-mesenchymal transition, similar to that induced by oncogenic V12Ras. Interestingly, while we identified a growth advantage to the ESX-P, Ets-2-P and V12Ras-P cells in 2D culture in growth restrictive conditions, these same cells had significantly reduced proliferative capacity in 3D culture. This observation suggests that the cell microenvironment may regulate a switch between mitosis and cell motility in transformed MCF-12A cells, an observation that may have potential clinical significance. Specifically, in vivo, metastatic breast cancer cells reside in a milieu similar to the 3D culture conditions, and thus may be relatively hypoproliferative and resistant to chemotherapeutic agents targeting rapidly dividing cells.

Ets factors, particularly Ets-1, Ets-2 and Pea-3, have been implicated in mammary tumorigenesis (Baert et al., 1997; Benz et al., 1997; Dittmer & Nordheim, 1998; Gilles et al., 1997; Shepherd & Hassell, 2000; Shepherd et al., 2001; Span et al., 2002; Watabe et al., 1998). Recently, another Ets factor, PSE/PDEF, initially identified in prostate, has been shown to be a marker for metastatic breast cancer (Ghadersohi & Sood, 2001; Mitas et al., 2002). The most definitive reports to date demonstrate that loss of Ets factor function suppresses both mammary

tumor cell transformation and tumor formation. Expression of a dominant-negative Ets construct in several mammary epithelial tumor cell lines resulted in reversion of anchorage-independent cell growth and cellular invasiveness in vitro (Delannoy-Courdent et al., 1998; Sapi et al., 1998). In addition, bi-transgenic *ets-2* knock out/MMTV-PyMT mice displayed reduced mammary tumor progression (Neznanov et al., 1999) and bi-transgenic *pea3* knock out/ MMTV-*neu* mice revealed delayed mammary tumor onset and reduced multiplicity (Shepherd et al., 2001).

ESX is an ETS transcription factor family member that may be particularly relevant in breast cancer due to its epithelial-specific mode of expression. ESX maps to human chromosome 1q32.1 in a region that is amplified in up to 50% of early-stage breast cancers and in DCIS. In addition, ESX RNA is over-expressed in human breast cancer (Chang et al., 1997; Tymms et al., 1997). Similarly, we have identified increased ESX expression in chemically-induced rat mammary tumors (data not shown). We previously reported that ESX-nonexpressing MCF-12A cells, transiently transfected with an ESX expression vector, formed significantly more colonies than transfected control cells (Eckel et al., 2003). Conversely, transient transfection of either an anti-sense or dominant-negative ESX construct into ESX-positive T47D cells resulted in considerable reduction in colony formation of these cells (Eckel et al., 2003). The data presented here corroborate and extend our previous findings and show that ESX expression is sufficient to transform immortalized mammary epithelial cells to a highly aggressive, transformed phenotype.

Oncogenic cell transformation is correlated with growth factor independence, often due to establishment of autocrine loops that constitutively activate the MAPK pathway. For example, oncogenic Ras has been shown to establish EGF-related autocrine loop pathways by inducing TGF-alpha, amphiregulin and HB-EGF (Falco et al., 1990; Gangarosa et al., 1997). Here we show that the ability of ESX, Ets-2 and V12-Ras to confer EGF-independent growth to MCF-

12A cells correlates with constitutive activation of MAPK (Fig. 3). Notably, ESX, Ets-2 and V12-Ras were unable to confer the full mitogenic effects of exogenous EGF. For example, the total number of cells was 5-fold lower in the ESX, Ets-2 or V12Ras stables in the absence of EGF (~40,000) compared to the same cells in the presence of EGF (~200,000). One interpretation of these data is that EGF activates pleiotropic growth and survival pathways in MCF12-A cells, whereas ESX, Ets-2 or V12Ras may be activating a more restrictive response. Alternatively, EGF may activate the MAPK pathway transiently; whereas ESX, Ets-2 and V12-Ras activate MAPK persistently, which subsequently dampens the growth response. This type of differential proliferative response to transient vs persistent MAPK activation has been previously reported (Traverse et al., 1994).

While growth factor independence is a key event in early stages of cellular transformation, a hallmark of overt metastasis is the transition of a tumor cell from an epithelial to a mesenchymal phenotype. During embryonic development, conversions between epithelium and mesenchyme occur regularly to allow for morphogenesis (Cunha, 1994; Hay, 1995). However, in normal adult tissue, EMT occurs only in epithelial cells during pathological wound healing and metastasis (Hay, 1995). Here, we have determined that ESX, Ets-2 and V12Ras induce functional attributes of EMT in MCF-12A cells.

In this study, the EMT phenotypes of adhesion, motility and invasion were identified by multiple methodological approaches. The property of altered adhesion was directly detected by increased adhesion in the 90 min adhesion assay, and indirectly inferred by the ability of ESX-P, Ets-2-P and V12Ras-P cells to grow in soft agar independent of cell-cell contacts. Additionally, we observed formation of solid tumor-like organoids in the 3D assay. This is a significant observation because non-transformed mammary epithelial cells undergo cell death when contacts

with basement membrane proteins are lost (Blum et al., 1989; Boudreau et al., 1995; Li et al., 1987), resulting in the formation of hollow duct-like structures (Coucouvanis & Martin, 1995; Humphreys et al., 1996). By contrast, the ability of ESX-P, Ets-2-P and V12Ras-P cells to form solid 3D structures demonstrates a loss of this cell adhesion requirement. Previously published reports have shown that Ets factors regulate key adhesion molecules, such as integrins and cadherins (Gilles et al., 1997; Oda et al., 1999; Rodrigo et al., 1999; Takaoka et al., 1998).

The observed changes in adhesive properties in the ESX-P, Ets-2-P and V12-Ras-P cells are predictive of increased motility. Indeed, increased motility in the ESX-P, Ets-2-P and V12-Ras-P cells was detected by three independent assays: scrape-injury, transwell filter migration and 3D organoid development. In support of our observations that gain of Ets function induces motility, expression of dominant-negative Ets-1 in murine MMT mammary tumor cell line resulted in inhibition of cell motility and enhancement of cell adhesion as measured by loss of cell scattering (Delannoy-Courdent et al., 1998). Similarly, expression of a dominant-negative Ets-2 in human BT20 breast cancer cell line resulted in a loss of motility (Sapi et al., 1998). Consistent with the motile phenotype, the ESX-P, Ets-2-P and V-12Ras-P cells, but not control cells, showed formation of broad lamellipodia and filopodia, prominent membrane protrusions at the leading edge of motile cells (Fig. 7) (Lauffenburger & Horwitz, 1996; Stossel et al., 1999). Of note, ESX-P and Ets-2-P showed formation of lamellopodia, whereas motile V12-Ras-P cells showed primarily filopodia formation (Fig. 7). These distinct motile phenotypes suggest that Ets factors activate a different motility pathway than V12Ras. Candidate regulators of lamellipodia and filopdia are members of the Rho family of small GTPases; Rho, Rac and Cdc42 (Bar-Sagi & Hall, 2000). Specifically, activation of Rac has been shown to induce lamellipodia, implicating Rac as a downstream effector of both ESX and Ets-2 Ets transcription factors in MCF12A cells.

In order for breast tumor cells to invade local tissue and gain access to the lymphatics and circulatory systems, they must be able to clear a path through extracellular matrix barriers (Basset et al., 1993; Benaud et al., 1998; Duffy et al., 1999). Evidence for acquisition of an invasive phenotype in ESX-P, Ets-2-P and V12-Ras-P cells was generated using two distinct assays. In the transwell filter invasion assay, filter pores were occluded with gelatin so that secretion of gelatinase by ESX-P, Ets-2-P and V12-Ras-P cells was required for invasiveness (Fig. 8). In the 3D organoid assay, invasiveness of ESX-P, Ets-2-P and V12-Ras-P cells was measured by the ability of cells to disseminate from the primary organoids and invade into surrounding reconstituted basement membrane (Fig. 9B). Of relevance to our observation that ESX and Ets-2 increase invasiveness of MCF12A cells, the Ets proteins Ets-1, ER81, PEA3, and E1AF have been shown to regulate a repertoire of genes that govern invasiveness in epithelial and mesenchymal cells, including collagenase, urokinase, matrylysin, and MT1-MMP (Shepherd & Hassell, 2000). Taken together, these data reveal a step-wise progression in tumor-like organoid development, manifested by the initial formation of large, solid 3D structures, where internal cells failed to die, followed by the formation of a peripheral zone of migrating and invasive cells that have acquired the EMT phenotype.

Finally, we provide evidence that in the physiologically-relevant environment of the 3D culture on reconstituted basement membrane, transformed MCF-12A cells significantly down-regulate mitosis in comparison to nontransformed cells. In addition, cells that had undergone an EMT were not observed to synthesize DNA, implying that a switch between mitogenesis and motogenesis occurs in 3D culture. Suppression of mitosis in epithelial cells that have undergone an EMT has been previously reported. Rat bladder carcinoma NBT-II cells transition to a mesenchymal phenotype when treated with acidic fibroblast growth factor (αFGF) (Savagner et

al., 1994). When NBT-II cells are simultaneously treated with αFGF and growth media, these cells failed to incorporate 3H-thymidine. Furthermore, in the scrape-wounding assay, NBT-II cells located at the edge of the wound underwent EMT and did not synthesize DNA, whereas confluent cells within the monolayer synthesized DNA. More recently, it has been demonstrated that FGF can stimulate cell movement in all phases of the cell cycle except G2 and M, further supporting a role for a molecular switch between mitosis and motility (Bonneton et al., 1999). Our observation that ESX-P, Ets-2-P and V12Ras-P cells are preferentially motogenic in 3D culture may have clinical impact. Specifically, tumorigenic cells that have undergone an EMT may be particularly resistant to standard chemotherapeutic drugs that target actively dividing cells.

FIGURE LEGENDS

Fig 1. Expression of ESX in wild-type MCF-12A and ESX-P cells. (A) MCF-12A cells fail to express ESX mRNA. Reverse transcriptase-polymerase chain reaction (RT-PCR) products of total RNA derived from MCF-7 (lanes 1-4) and MCF-12A (lanes 5-8) human breast cells, using ESX-specific primers, were submitted to 1% agarose gel electrophoresis. Samples were removed after 20 (lanes 1 & 5), 25 (lanes 2 & 6), 30 (lanes 3 & 7), and 35 (lanes 4 & 8) PCR cycles. DNA size markers are indicated on the left. The expected ESX band of 1.1 kb is indicated by an arrow and primer-dimer band denoted by a small arrow. **(B)** RT-PCR analysis of HA-ESX expression in MCF-12A stable pools. RT-PCR was performed on RNA isolated from ESX-P, Ets-2-P and V12Ras-P stable pools, as described in Materials and Methods. Twenty-five cycles of PCR were carried out using oligonucleotides primers specific for exogenous HA-ESX. The PCR products were loaded onto a 1% agarose gel, electrophoresed and stained with ethidium bromide. Lane 1: H_2O-only control; lane 2: minus RT; lane 3: MCF12-A; lane 4: pCGN2-P; lane 5: ESX-P; lane 6: Ets-2-P; lane 7: V12-Ras-P; and lane 8: pCGN2-HA-ESX plasmid as positive control.

Fig 2. ESX-P, Ets-2-P and V12Ras-P cells demonstrate enhanced EGF-independent cell growth. Cell growth of wild-type and pCGN2-P, ESX-P, Ets-2-P and V12Ras-P stable cell lines were determined in media containing reduced serum (1% horse serum) in the absence of EGF (upper panel) or in the presence of 20 ng/ml EGF (lower panel). Cells were plated at an initial density of 10,000 cells per plate. At 24-hr intervals, cells were harvested from plates and manually counted in triplicate using a hemocytometer, for a total of five days. Data represent mean cell counts +/- SEM.

Fig 3. ESX-P, Ets-2-P and V12Ras-P stable cell lines exhibit elevated levels of activated p44/42 MAP kinase in the absence of EGF. Wild-type and pCGN2-P, ESX-P, Ets-2-P and V12Ras-P stable cell lines were serum-starved for 12 hours in media containing 0.1% horse serum and lacking EGF. Cell lysates were prepared from wild type MCF-12A cells (lane 1), vector-only stable cells (lane 2) and stable cell lines expressing either HA-ESX (lane 3), HA-Ets-2 (lane 4) or V12-Ras (lane 5). Equal amounts of total cellular protein were electrophoresed on 10% PAGE and analysed by Western blot. Upper panel depicts a representative Western blot probed with an antibody specific for phosphorylated p44/42 MAPK (pMAPK). Lower panel depicts the same Western blot stripped and re-probed with an antibody against β-actin (Actin), to control for loading differences between samples.

Fig 4. Colony formation assay of stable pCGN2-P, ESX-P, Ets-2-P and V12Ras-P cells in soft agar. Twenty thousand cells from each cell line were plated in soft agar. Representative photographs taken at four weeks show colonies or the lack thereof for pCGN2 control vector (upper left), HA-ESX (upper right), HA-Ets-2 (lower left) and V12Ras (lower right) transfected stable cell lines. Size bar equals 2 mm.

Fig 5. Cell adhesion is altered in ESX-P, Ets-2-P and V12Ras-P cells. Ability of cells to adhere to plastic substratum was measured over a 75 min time course. Adherent cells were stained with 0.1% crystal violet and dye extracted with ethanol. Adherent cell number was quantified by determining optical absorbance at 590 nm. Bars represent % adherent cells at indicated time points after initial plating. Experimental conditions were performed in triplicate and data are expressed as mean +/- SEM. ESX-P, Ets-2-P and V12Ras-P cells revealed

significantly increased adherence at 75 min post-plating compared to vector control cells, $p<0.008$, 0.001 and 0.006, respectively, (2-tailed t-test).

Fig 6. Increased cell motility in ESX-P, Ets-2-P and V12Ras-P cells . (A) Cell motility was increased in ESX-P, Ets-2-P and V12Ras-P cells in the scrape assay. Cells in 2-D culture were wounded by scraping confluent monolayers. The ability of the cells to re-populate the scrape zone in the presence of media devoid of serum and growth factors was determined after 24 hr. pCGN2-P (upper left panel), ESX-P cells (upper right panel), Ets-2P cells (lower left panel) and V12Ras-P cells (lower right panel). The pCGN2-P cell monolayer consisted of two distinct cell populations (upper left), fine arrow depicts elongated fibroblast-like cells and wide arrows depict dense, epithelial like colonies. Experimental conditions performed in triplicate, experiment in duplicate. Representative data shown. Size bar equals 100 μm. **(B)** Migration of cells through Boyden chamber filters was increased in ESX-P, Ets-2-P and V12Ras-P cells. Filters with 8 μm pores were coated with 10 μg/ml gelatin. Cells were plated in upper wells of chambers using 0.5% FBS as a chemo-attractant in lower wells. Cell motility was measured as a function of the number of cells that traversed from the upper chamber to lower chamber within 4 hr. Data are expressed as mean +/- SEM. ESX-P, Ets-2-P, and V12Ras-P cells displayed significantly higher motility than pCGN2-P control cells, $p<0.0001$ for all three cell lines (two-tailed t test). Experimental conditions performed in triplicate, experiment in duplicate. While Fig. 6B depicts a representative experiment performed in triplicate, the same trends in motility observed for the ESX-P, Ets-2-P and V12-Ras-P cells were reproducibly obtained in three separate experiments

Fig 7. Motile ESX-P and Ets-2-P cells predominantly display lamellopodia, while V12Ras cells display filopodia. Cells that traversed the 8 μm filter in the transwell filter motility assay were stained with 0.1% crystal violet and representative areas photographed. Upper left panel shows a single migratory CGN2-P cell and numerous empty 8 μm filter pores (pore denoted by arrow). Actively motile ESX-P cells (upper right panel) displayed prominent lamellopodia (arrow). Motile Ets-2-P cells (lower left panel), displayed both ruffled lamellopodia (arrow) and filopodia, while motile V12Ras-P cells (lower right panel) displayed prominent filopodia (arrow). Size bar equals 50 μm.

Fig 8. Invasion through modified Boyden chamber filters is increased in ESX-P, Ets-2-P and V12Ras-P cells. Eight μm filter pores were occluded with 200 μg/ml gelatin. Cells were plated in upper wells of chambers using 0.5% FBS as a chemo-attractant in lower wells. Cell transit from upper chamber to lower chamber requires degradation of gelatin within pores. Cell invasion was measured as the number of cells that traversed through filter pores within 24 hr. Data are expressed as mean +/- SEM. ESX-P, Ets-2-P, and V12Ras-P cells displayed significantly higher invasiveness than pCGN2-P control cells, $p<0.0001$ for all three cell lines (two-tailed t test). Experimental conditions performed in triplicate, experiment in duplicate. the invasion results of the four stable cell lines in serum-free and EGF-free culture medium, either in the presence (moderately restrictive media) or absence (highly restrictive media) of insulin, hydrocortisone and cholera toxin.

Fig 9. Wild-type MCF-12A cells form mammary-like organoids in 3D culture, while ESX-P, Ets-2-P and V12Ras-P cells form tumor-like structures displaying a functional epithelial-

to-mesenchymal transition (EMT). (A) MCF 12A and pCGN-2-P cells recapitulate aspects of mammary gland development in 3D culture. MCF12A and vector control pCGN2-P cells were overlaid onto thick, reconstituted EHS basement membrane as single cell suspensions. Single cell aggregation into organoids was monitored for 72 hr and organoids processed for 5 μm histological sections and stained with hematoxylin and eosin. Left three panels depict typical organoid morphologies observed with MCF 12A cells. Upper left panel shows an alveolar-like structure with hollowed lumen (asterisks) and evidence of an internal apoptotic cell (arrow), 400X. Middle left panel shows hollowed duct-like organoid, 400X, and lower left panel shows high magnification view of a duct-like structure demonstrating morphological evidence of cell polarity, cell-cell junctions and an apoptotic cell within the lumen (arrow), 1000X. Right three panels depict typical organoid morphologies observed with vector control pCGN-2-P cells. Upper right panel shows duct-like structure with partial cavitation, 400X. Middle right panel shows hollowed duct-like structure, 400X and lower right panel shows high magnification view of duct-like structure, 1000X. Size bar in 400X photos equals 25 μm and in 1000X photos equals 10 μm. **(B)** ESX-P, Ets-2-P and V12Ras-P cells form solid tumor-like structures and fail to organize into mammary gland-like structures in 3D culture. ESX-P, Ets-2-P and V12Ras-P cells were cultured and processed as described in Fig. 9A. Top panel and three left panels depict typical solid tumor-like organoids formed by ESX-P, Ets-2-P and V12Ras-P cells at 24 hr respectively, 400X. Right three panels show evidence of epithelial to mesenchymal transition in ESX-P, Ets-2-P and V12Ras-P cells at periphery of organoids after 72 hr in culture. Arrowheads identify invasive, fibroblast-like cells that penetrate into surrounding matrices. Size bar in 400X photos equals 25 μm and in 1000X photos equals 10 μm.

Fig 10. BrdU incorporation into pCGN2-P, ESX-P, Ets-2-P and V12Ras-P cells in 3D culture. (A) Immunohistochemical detection of BrdU of pCGN2-P, ESX-P, Ets-2-P and V12Ras-P cells in 3D culture. pCGN2-P, ESX-P, Ets-2-P and V12Ras-P cells were overlaid onto thick reconstituted basement membrane as single cell suspensions. After 72 hr in culture, cells were treated with 1mM BrdU for 24 hr. pCGN2-P cells (upper left) form numerous small duct-like structures (asterisk) with frequent brown staining, BrdU-positive cells (arrow). ESX-P (upper right), Ets-2-P (lower, left) and V12Ras-P (lower right) cells form disorganized, solid tumor-like organoids with few BrdU-positive cells (arrows). Invasive cells are observed to penetrate surrounding matrices (arrowheads). Experimental conditions were each performed in quadruplicate, and entire experiment in duplicate. Size bar equals 25 μm. **(B)** Quantitation of BrdU incorporation. Proliferative index was determining by quantifying BrdU incorporation between 72 and 96 hr post plating, as described in Materials and Methods. Experimental conditions were each performed in quadruplicate, and entire experiment in duplicate. Data are expressed as mean percentage of positive cells +/- SEM. Asterisk indicates statistically different from vector control cells, $p < 0.01$, Poisson regression, adjusted for multiple comparisons.

REFERENCES

Baert, J., Monte, D., Musgrove, E., Albagli, O., Sutherland, R. & Delaunoit, Y. (1997). *Int. J. Cancer*, **70,** 590-597.

Bar-Sagi, D. & Hall, A. (2000). *Cell*, **103,** 227-238.

Basset, P., Wolf, C. & Chambon, P. (1993). *Breast Cancer Res Treat*, **24,** 185-193.

Bemis, L.T. & Schedin, P. (2000). *Cancer Res.*, **60,** 3414-3418.

Benaud, C., Dickson, R. & Thompson, E. (1998). *Breast Cancer Res Treat*, **50,** 97-116.

Benz, C., O'Hagan, R., Richter, B., Scott, G., Chang, C.-H., Xiong, X., Chew, K., Ljung, B.-M., Edgerton, S., Thor, A. & Hassell, J. (1997). *Oncogene*, **15,** 1513-1525.

Bernhardt, G., Reile, H., Birnbock, H., Spruss, T. & Schoenberger, H. (1992). *J. Cancer Res. clin.Oncol.*, **118,** 35-43.

Blum, J.L., Ziegler, M.E. & Wicha, M.S. (1989). *Environ. Health Perspect.*, **80,** 71-83.

Bonneton, C., Sibarita, J.B. & Thiery, J.P. (1999). *Cell Motil. Cytoskeleton*, **43,** 288-295.

Boudreau, N., Sympson, C.J., Werb, Z. & Bissell, M.J. (1995). *Science*, **267,** 891-893.

Bradford, A.P., Brodsky, K.S., Diamond, S.E., Kuhn, L.C., Liu, Y. & Gutierrez-Hartmann, A. (2000). *J. Biol. Chem.*, **275,** 3100-3106.

Chang, C., Scott, G., Kuo, W., Xiong, X., Suzdaltseva, Y., Park, J., Sayre, P., Erny, K., Collins, C., Gray, J. & Benz, C. (1997). *Oncogene*, **14,** 1617-1622.

Chang, C.-H., Scott, G.K., Baldwin, N.A. & Benz, C.C. (1999). *Oncogene*, **18,** 3682-95.

Coucouvanis, E. & Martin, G.R. (1995). *Cell*, **83,** 279-287.

Cunha, G.R. (1994). *Cancer*, **74,** 1030-1044.

Delannoy-Courdent, A., Mattot, V., Fafeur, V., Fauquette, W., Pollet, I., Calmels, T., Vercamer, C., Boilly, B., Vandenbunder, B. & Desbiens, X. (1998). *J. Cell Sci.*, **111,** 1521-1534.

Dittmer, J. & Nordheim, A. (1998). *Bioch. Biophys. Acta*, **1377,** F1-F11.

Donaldson, L., Petersen, J., Graves, B. & McIntosh, L. (1994). *Biochemistry*, **33,** 13509-13516.

Donaldson, L., Petersen, J., Graves, B. & McIntosh, L. (1996). *EMBO J.*, **15,** 125-134.

Duffy, M., Maguire, T., McDermott, E. & O'Higgins, N. (1999). *J Surg Oncol*, **71,** 130-135.

Eckel, K.L., Tentler, J.J., Diamond, S.E., Cappetta, G.J. & Gutierrez-Hartmann, A. (2003). *DNA & Cell Biol.*, **22,** 79-94.

Falco, J., Baylin, S., Lupu, R., Borges, M., Nelkin, B., Jasti, R., Davidson, N. & Mabry, M. (1990). *J Clin Invest*, **85,** 1740-1745.

Gangarosa, L.M., Sizemore, N., Graves-Deal, R., Oldham, S.M., Der, C.J. & Coffey, R.J. (1997). *J Biol Chem*, **272,** 18926-31.

Ghadersohi, A. & Sood, A.K. (2001). *Clin Cancer Res*, **7,** 2731-8.

Gilles, C., Polette, M., Birembaut, P., Brunner, N. & Thompson, E. (1997). *Clin. Exp. Metastasis*, **15,** 519-526.

Graves, B. & Petersen, J. (1998). *Advances in Cancer Research.* Klein, G. (ed.).

Hanahan, D. & Weinberg, R.A. (2000). *Cell*, **100,** 57-70.

Hay, E.D. (1995). *Acta Anat.*, **154,** 8-20.

Horwitz, A.F., Sandborg, R.R. & Huttenlocher, A. (1995). *Curr. Op. Cell Biol.*, **7,** 697-706.

Humphreys, R.C., Krajewska, M., Krnacik, S., Jaeger, R., Weiher, H., Krajewski, S., Reed, J.C. & Rosen, J.M. (1996). *Development*, **122,** 4013-4022.

Kantor, J.D. & Zetter, B.R. (1996). *Mammary tumor cell cycle, differentiation and metastasis.* Dickson, R. & Lippman, M. (eds). Klewer Academic Publishers: New York, pp 303-323.

Kordon, E.C. & Smith, G.H. (1998). *Development*, **125,** 1921-1930.

Lauffenburger, D. & Horwitz, A. (1996). *Cell*, **84,** 359-369.
Leprince, D., Gegonne, A., Coll, J., deTaisne, D., Schneeberger, A., Largrou, C. & Stehelin, D. (1983). *Nature*, **306,** 395-397.
Li, M.L., Aggeler, J., Farson, D.A., Hatier, C., Hassell, J. & Bissell, M.J. (1987). *Proc. Natl. Acad. Sci. USA*, **84,** 136-140.
Liu, E., Thor, A., He, M., Barcos, M., Ljung, B. & Benz, C. (1992). *Oncogene*, **7,** 1027-1032.
Mitas, M., Mikhitarian, K., Hoover, L., Lockett, M.A., Kelley, L., Hill, A., Gillanders, W.E. & Cole, D.J. (2002). *Br J Cancer*, **86,** 899-904.
Neznanov, N., Man, A., Yamamoto, H., Hauser, C., Cardiff, R. & Oshima, R. (1999). *Cancer Research*, **59,** 4242-4246.
O'Hagan, R. & JA, H. (1998). *Oncogene*, **16,** 301-310.
Oda, N., Abe, M. & Sato, Y. (1999). *J. Cell. Physiol.*, **178,** 121-132.
Oettgen, P., Alani, R., Barcinski, M., Brown, L., Akbarali, Y., Boltax, J., Kunsch, C., Munger, K. & Libermann, T. (1997). *Mol. Cell. Biol.*, **17,** 4419-4433.
Paine, T.M., Soule, H.D., Pauley, R.J. & Dawson, P.J. (1992). *International Journal of Cancer*, **50(3),** 463-473.
Rodrigo, I., Cato, A. & Cano, A. (1999). *Exp. Cell. Res.*, **248,** 358-371.
Sapi, E., Flick, M., Rodov, S. & Kacinski, B. (1998). *Cancer Res.*, **58,** 1027-1033.
Savagner, P., Boyer, B., Valles, A.M., Jouanneau, J. & Thiery, J.P. (1994). *Cancer Treat. Res.*, **71,** 229-249.
Schedin, P., Mitrenga, T. & Kaeck, M. (2000). *J. Mammary Gland Biol. Neoplasia*, **5,** 211-225.
Shepherd, T. & Hassell, J. (2000). *J. Mammary Gland Biol. Neoplasia*, **6,** 129-140.
Shepherd, T.G., Kockeritz, L., Szrajber, M.R., Muller, W.J. & Hassell, J.A. (2001). *Curr. Biol.*, **11,** 1739-1748.
Span, P.N., Manders, P., Heuvel, J.J., Thomas, C.M., Bosch, R.R., Beex, L.V. & Sweep, C.G. (2002). *Oncogene*, **21,** 8506-9.
Stossel, T., Hartwig, J., Janmey, P. & Kwiatkowski, D. (1999). *Biochem. Soc. Symp.*, **45,** 267-280.
Takaoka, A., Yamada, T., Gotoh, M., Kanai, Y., Imai, K. & Hirohashi, S. (1998). *J. Biol. Chem.*, **273,** 33848-33855.
Traverse, S., Seedorf, K., Paterson, H., Marshall, C.J., Cohen, P. & Ullrich, A. (1994). *Curr. Biol.*, **4,** 694-701.
Tymms, M., Ng, A., Thomas, R., Schutte, B., Zhou, J., eyre, H., Sutherland, G., Seth, A., Rosenberg, M., Papas, T., Debouck, C. & Kola, I. (1997). *Oncogene*, **15,** 2449-2462.
Wang, B., Soule, H.D. & Miller, F.R. (1997). *Anticancer Research*, **17,** 4387-4394.
Wasylyk, B., Hagman, J. & Gutierrez-Hartmann, A. (1998). *Trends Biochem. Sci.*, **23,** 213-216.
Watabe, T., Yoshida, K., Shindoh, M., Kaya, M., Fujikawa, K., Sato, H., Seiki, M., Ishii, S. & Fujinaga, K. (1998). *Int. J. Cancer*, **77,** 128-137.
Weaver, V.M., Fischer, A.H., Peterson, O.W. & Bissell, M.J. (1996). *Biochem. Cell Biol.*, **74,** 833-851.

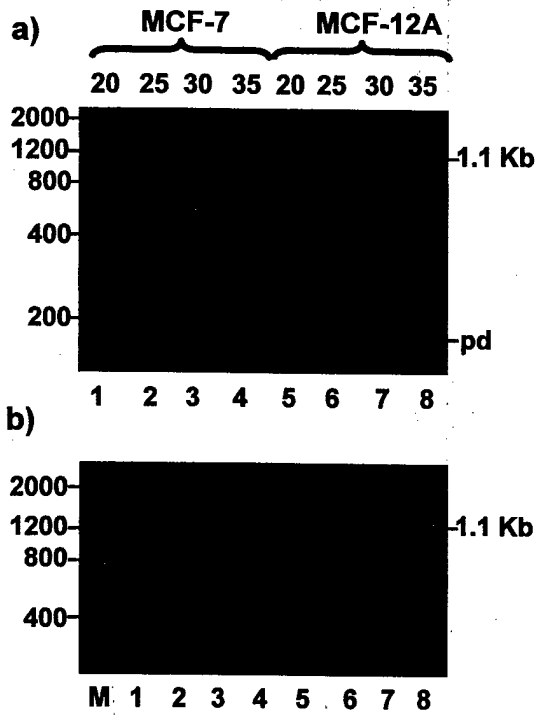
a)
MCF-7
MCF-12A
20 25 30 35 20 25 30 35
2000
1200
800
400
200
1.1 Kb
pd
1 2 3 4 5 6 7 8
b)
2000
1200
800
400
1.1 Kb
M 1 2 3 4 5 6 7 8

a)

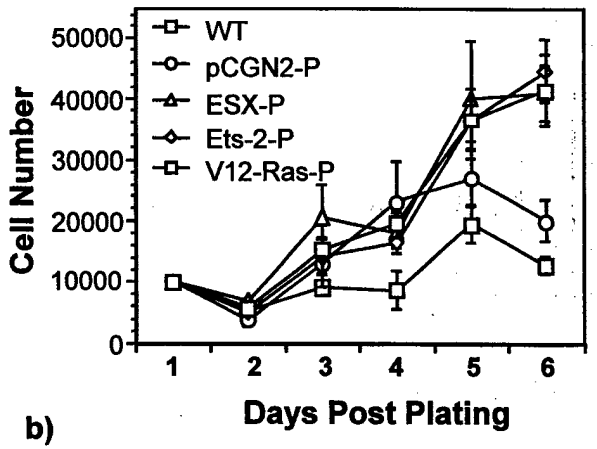
WT
pCGN2-P
ESX-P
Ets-2-P
V12-Ras-P
Cell Number
50000
40000
30000
20000
10000
0
1
2
3
4
5
6
Days Post Plating

b)

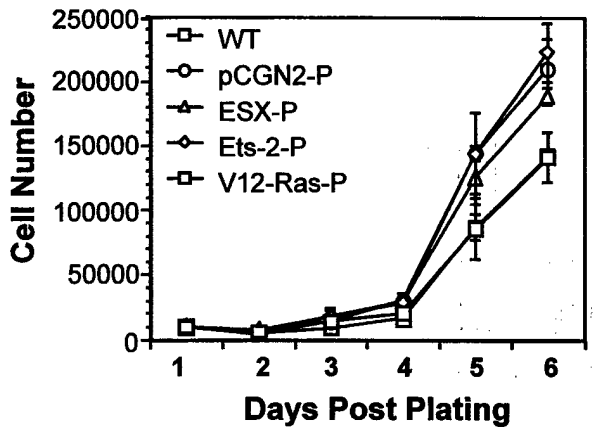
WT
pCGN2-P
ESX-P
Ets-2-P
V12-Ras-P
Cell Number
250000
200000
150000
100000
50000
0
1
2
3
4
5
6
Days Post Plating

pMAPK
Actin
MCF12 A
pCGN2-P
ESX-P
Ets-2-P
V12Ras-P

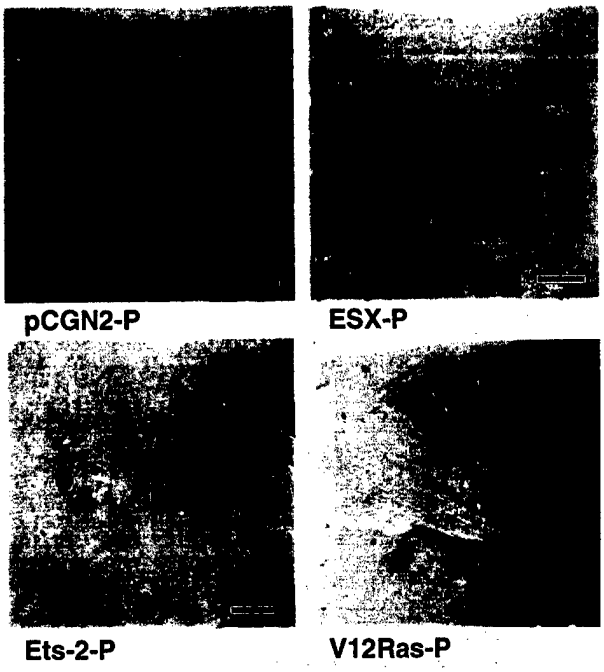
pCGN2-P
ESX-P
Ets-2-P
V12Ras-P

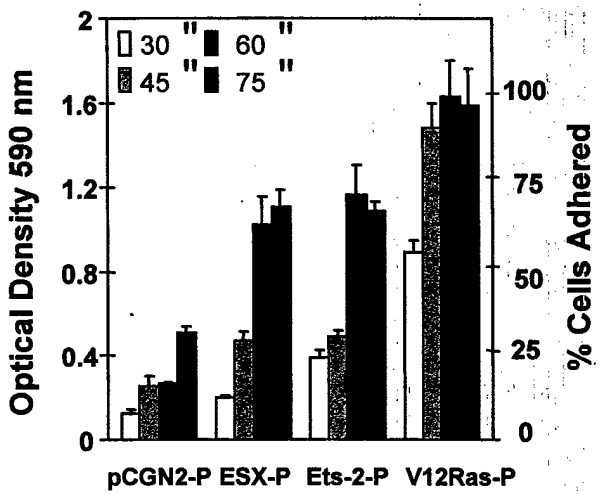
Optical Density 590 nm
2
1.6
1.2
0.8
0.4
0
30 "
45 "
60 "
75 "
100
75
50
25
0
% Cells Adhered
pCGN2-P
ESX-P
Ets-2-P
V12Ras-P

a)

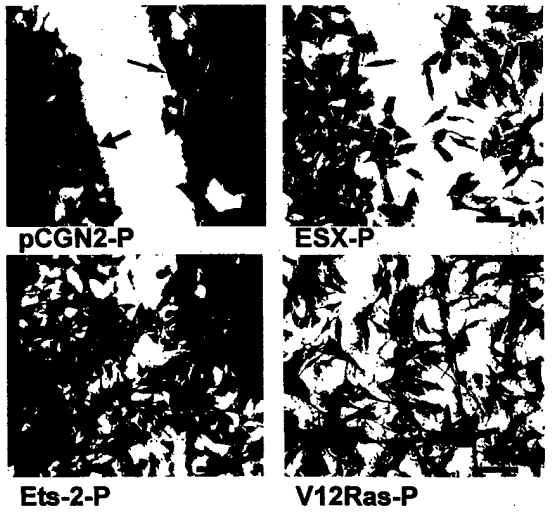
pCGN2-P
ESX-P
Ets-2-P
V12Ras-P

b)

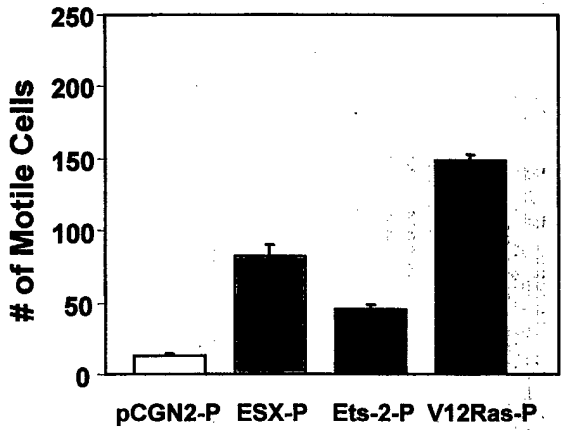
# of Motile Cells
250
200
150
100
50
0
pCGN2-P
ESX-P
Ets-2-P
V12Ras-P

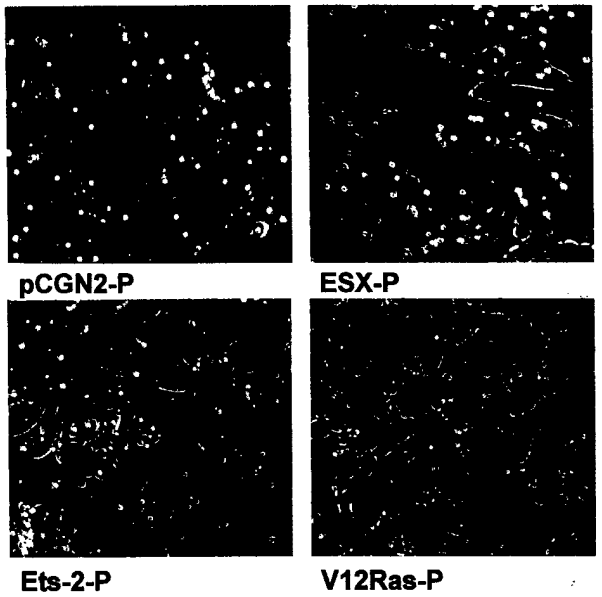
pCGN2-P
ESX-P
Ets-2-P
V12Ras-P

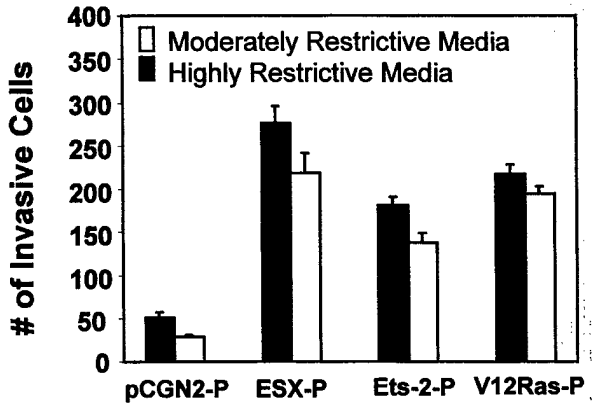
Moderately Restrictive Media
Highly Restrictive Media
# of Invasive Cells
400
350
300
250
200
150
100
50
0
pCGN2-P
ESX-P
Ets-2-P
V12Ras-P

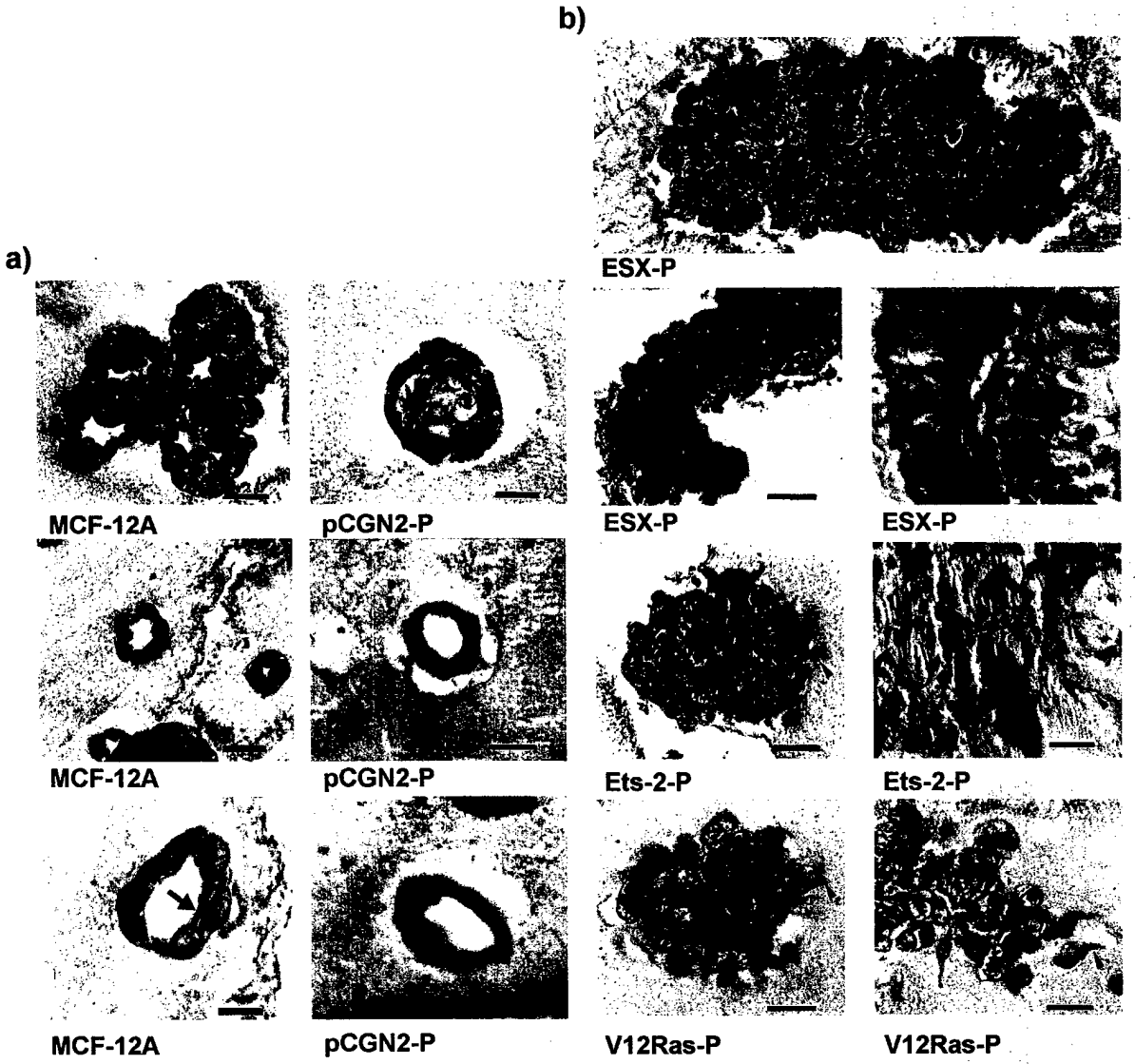
a)
b)
ESX-P
MCF-12A
pCGN2-P
ESX-P
ESX-P
MCF-12A
pCGN2-P
Ets-2-P
Ets-2-P
MCF-12A
pCGN2-P
V12Ras-P
V12Ras-P

a)

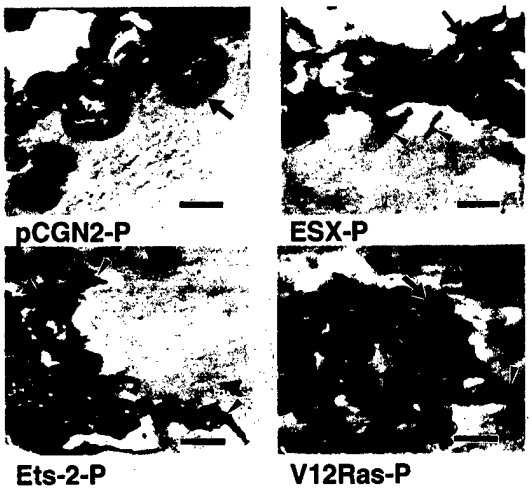
pCGN2-P
ESX-P
Ets-2-P
V12Ras-P

b)

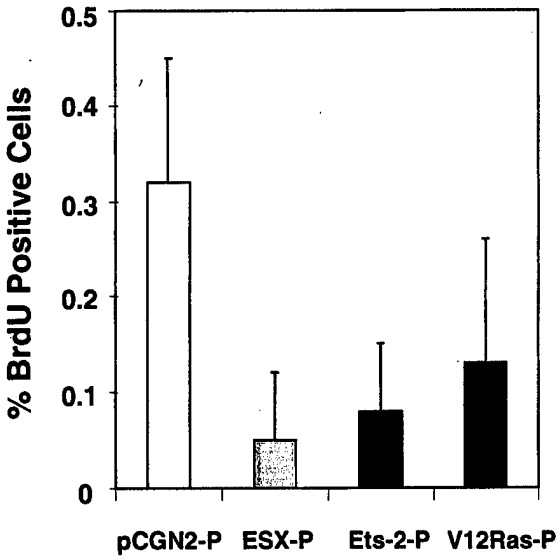
% BrdU Positive Cells
0.5
0.4
0.3
0.2
0.1
0
pCGN2-P
ESX-P
Ets-2-P
V12Ras-P